

DTIC FILE COPY

2

GL-TR-90-0307

New Version of NASA-Ames/Jamieson Science
and Engineering Point Source Infrared Sky Model

Martin Cohen

Jamieson Science & Engineering, Inc.
5321 Scotts Valley Drive, Suite 204
Scotts Valley, CA 95066

8 January 1991

Final Report
Period Covered: 13 June 1989 - 12 October 1990

Approved for public release; distribution unlimited


GEOPHYSICS LABORATORY
AIR FORCE SYSTEMS COMMAND
UNITED STATES AIR FORCE
HANSCOM AIR FORCE BASE, MASSACHUSETTS 01731-5000

DTIC
ELECTE
FEB 25 1991
S D D

AD-A231 953

91 2 22 053

"This technical report has been reviewed and
is approved for publication"



DAVID S. AKERSTROM
CONTRACT MANAGER

STEPHAN D. PRICE
BRANCH CHIEF

FOR THE COMMANDER



R. EARL GOOD
DIVISION DIRECTOR

This report has been reviewed by the ESD Public Affairs Office (PA) and is releasable to the National Technical Information Service (NTIS).

Qualified requestors may obtain additional copies from the Defense Technical Information Center. All others should apply to the National Technical Information Service.

If your address has changed, or if you wish to be removed from the mailing list, or if the addressee is no longer employed by your organization, please notify GL/DAA, Hanscom AFB, MA 01731. This will assist us in maintaining a current mailing list.

Do not return copies of this report unless contractual obligations or notices on a specific document requires that it be returned.

REPORT DOCUMENTATION PAGE

Form Approved
OMB No 0704-0188

Public reporting burden for this collection of information is estimated to average 1 hour per response, including the time for reviewing instructions, searching existing data sources, gathering and maintaining the data needed, and completing and reviewing the collection of information. Send comments regarding this burden estimate or any other aspect of this collection of information, including suggestions for reducing this burden, to Washington Headquarters Services, Directorate for Information Operations and Reports, 1215 Jefferson Davis Highway, Suite 1204, Arlington, VA 22202-4302, and to the Office of Management and Budget, Paperwork Reduction Project (0704-0188) Washington, DC 20503.

1. AGENCY USE ONLY (Leave blank)		2. REPORT DATE 8 January 1991		3. REPORT TYPE AND DATES COVERED Final Report 13 Jun 1989-12 Oct 1990	
4. TITLE AND SUBTITLE New Version of NASA-Ames/Jamieson Science and Engineering Point Source Infrared Sky Model				5. FUNDING NUMBERS PE: 63220C PR S321 TA 18 WU AF	
6. AUTHOR(S) Martin Cohen				Contract F19628-89-C-0116	
7. PERFORMING ORGANIZATION NAME(S) AND ADDRESS(ES) Jamieson Science & Engineering, Inc 5321 Scotts Valley Drive, Suite 204 Scotts Valley, CA 95066				8. PERFORMING ORGANIZATION REPORT NUMBER	
9. SPONSORING/MONITORING AGENCY NAME(S) AND ADDRESS(ES) Geophysics Laboratory Hanscom AFB, MA 01731-5000 Contract Manager: Stephan Price/OPC				10. SPONSORING/MONITORING AGENCY REPORT NUMBER GL-TR-90-0307	
11. SUPPLEMENTARY NOTES					
12a. DISTRIBUTION / AVAILABILITY STATEMENT Approved for public release; distribution unlimited				12b. DISTRIBUTION CODE	
13. ABSTRACT Our existing Sky Model for the point source infrared sky is extended to make predictions for any filter lying wholly within the range 2.0 to 35.0 μm . To support this extension we have developed a library of complete 2-35 μm low-resolution (0.1 μm step size) spectra to represent the 87 categories of Galactic object and 4 types of extragalactic source implicit in the Model. This library is based upon the technique of the "spectral template" whereby existing spectral fragments for individual sources (from ground-based, airborne, and satellite-borne instruments) are combined into complete spectra. Templates provide a natural way of representing the complete spectral energy distributions of celestial sources for which only infrared photometry or partial spectroscopy exists, provided that such sources can be classified by the scheme inherent in the Sky Model which is essentially based upon the combination of optical and mid-infrared attributes. Consequently, templates bear upon the important general problem of establishing mid-infrared calibration sources. The new Model is validated by comparison with broadband K (2.2 μm) source counts.					
14. SUBJECT TERMS celestial backgrounds - infrared point sources - sky model				15. NUMBER OF PAGES 52	
				16. PRICE CODE	
17. SECURITY CLASSIFICATION OF REPORT Unclassified	18. SECURITY CLASSIFICATION OF THIS PAGE Unclassified	19. SECURITY CLASSIFICATION OF ABSTRACT Unclassified	20. LIMITATION OF ABSTRACT SAR		

I. INTRODUCTION

This report describes an extension of the Sky Model for the point source infrared sky presented by Wainscoat et al. (1990: hereafter WCVWS; see also Cohen et al. 1990). The Model represents the sky by six geometrically distinct components: five Galactic (the exponential disk, bulge, halo, spiral arms, and molecular ring) and one extragalactic. Each component is modeled in substantial detail based upon pre-existing information drawn from optical, infrared, radio continuum, and radio molecular line surveys. It is intended to provide a picture of the point source sky, originally at mid-infrared wavelengths, that comprises sufficient realism to match all source counts currently available (dominantly from IRAS). Indeed, WCVWS demonstrate that the Model predicts source counts ($\log N, \log S$) that agree with observations extremely well (to within better than a factor of 2) across the entire sky at broadband 12 and 25 μm wavelengths. The match is well within a factor of 1.5 for most zones of the sky at high and intermediate Galactic latitudes. All specific disagreements can be traced to discrepancies between the analytic representation of the geometry of the Galaxy used in the Model and the real Galaxy (for example, warps in the neutral hydrogen distribution that make the spiral arms rise out of the Galactic plane: cf. WCVWS), or to uncertainties in the mid-infrared colors of bulge red giants. The reader is referred to WCVWS for detailed 12 and 25 μm validations of the Model by comparison with IRAS Point Source Catalog, Faint Source Survey, Serendipitous Survey, and the deep Hacking and Houck (1987) ecliptic pole survey. The success of these comparisons essentially vindicates the formalism of the Model code, the geometry of its components, and the critical selections from the literature of absolute magnitudes, scale heights, and population densities for the many categories of celestial source represented in it.

The work of WCVWS was primarily intended to apply to the mid-infrared range because the most abundant and detailed source counts of the infrared sky are those provided by IRAS. The Model comprises broadband infrared filters (J, H, K, [2.4], and IRAS 12 and 25 μm) and has the capacity to operate continuously for any filter lying entirely within the range of the IRAS Low Resolution Spectrometer (LRS), namely 7.67–22.74 μm . The restriction to the LRS wavelength range was necessary because the LRS instrument provides a homogeneous set of complete spectral representations for all the categories of celestial source implicit in the Model's source table. To go outside the LRS range would have demanded a far greater effort solely on the detailed construction of these spectra, with correspondingly less time available for the development of the physical realism of the Model.

It is the purpose of this report to remove this restriction to the LRS range and to extend the validity of the Model to the complete 2.0–35.0 μm range. Section II deals with the concept of infrared spectral templates and their value to the library from which the Model draws its continuous spectral information. Section III describes the construction of templates in detail. As a consequence of the extension in spectra range, some of the absolute B, V, J, H, 2.2, and 2.4 μm magnitudes used in the source table (cf. WCVWS) have been revised. These changes are described in Section IV. Section V compares the new Model's predictions with several 2.2 μm surveys of point sources.

The new version of the Sky Model is capable of providing information of material assistance to the planning of future infrared space surveys



on For	
RAAI	
5	
need	
ation	
ation/	
bility Codes	
ail and/or	
Special	

Dist

A-1

because it can predict, across the sky, the expected density of sources at different flux levels and in different passbands.

II. SPECTRAL TEMPLATES

The categories of celestial source represented in the Model include both optically known normal stars and nonstellar objects, and the highly evolved red giants of both carbon- and oxygen-rich sequences, that are extremely luminous at mid-infrared wavelengths. Each category has an associated complete LRS spectrum within a library which the Model draws upon when needed. The extension to the 2-35 μm realm, therefore, hinges upon the replacement of the library of LRS spectra by a set of complete 2-35 μm spectra for all celestial categories.

Such a library must include an extremely diverse range of objects, from normal hot dwarf stars through cool dusty giants, and optically-invisible dust-enshrouded AGB objects to planetary and reflection nebulae, HII regions, and even galaxies. Consequently, the approach we favor for the construction of the library is a semi-empirical one, based upon the extraction from the literature of fragments of real spectra obtained for a wide variety of infrared sources, by different instruments, and in several spectral regions. The alternative is an analytic approach in which we require a theoretical understanding of the infrared spectral energy distributions of all these diverse sources across the entire spectral range (for example, by adopting a specific source of opacity for a narrow range of stellar types: G to early M, cf. Engelke 1990).

The first step in our procedure involves the identification of specific individual objects to represent each of the many spectral categories used in the Model. Ideally, to accommodate natural dispersion in properties, one would like to select a minimum of two sources per celestial category, although this is not always possible for extremely rare categories. Table 1 summarizes the categories of source required by the Model; the objects chosen to represent these categories for which at least partial infrared spectral information exists; and the references for the fragments available.

The second step necessitates the acquisition of digital files of these spectral fragments either by scanning of the published spectra (or larger scale versions thereof, provided by the authors) or by direct electronic transmission by the original observers. By this means, ~500 fragments representing ~177 separate sources were accumulated. Spectral fragments can be divided naturally into several classes depending on the spectral regime; these natural divisions also represent distinctions by detector technology and observing site (ground-based or airborne or satellite-borne). To give an impression of the availability of fragments in different regions, Table 2 summarizes the total database of spectral fragments assembled in Table 1, broken down by wavelength region. The natural divisions are: 2-4/5; 5-8; 8-13; 7.7-22.7 (the LRS); 15-30; >30 μm . From this, one clearly recognizes both the relative scarcity of the airborne fragments and their importance to the complete spectra.

Next comes the combination of fragments into complete spectra with appropriate actions to be taken in the complete absence of data in specific regions, and with corrections to be made for photospheric absorptions that might not have been observed in all sources. These details constitute section III.

The separate, complete spectra on individual sources in a common category must be corrected for purely interstellar extinction, rendering

them intrinsic spectra, then normalized, and finally averaged together, yielding the category's template. We implicitly assume that every source of a particular category may be well represented by the average intrinsic template created from the spectra of the elemental sources used to construct the average. In this way, the complete library can be constructed.

We note that the concept of these templates is relevant to the general problem of absolute calibration for airborne and spaceborne infrared detectors in the mid- and long-wavelength-infrared regime. The problem is to establish standards for a particular flight series or satellite mission that lie within a specific region of the sky and emit strongly within a specific region in the infrared. While there may exist bright sources with the required positions and wavelength coverage, there often is a complete absence of any continuous spectral information on these same sources even at low resolution. If a source can be categorized in the context of the Sky Model, it can be represented by a unique spectral template. All that is required is to normalize that template to match the best broadband photometry available on the individual source. This provides at least a first approximation to an absolute calibration for the source. The template technique has been applied in this context to relatively normal stars, typically K and early M giants (Walker and Cohen 1989). However, the present report describes the first broad application of the method to a wide variety of sources and is built from a much larger database of fragments than previously available. We offer these templates as a pro tem solution to the general demands of mid-infrared calibration.

III. METHODOLOGY

a) Digitization of spectral fragments

Unless spectral data were transmitted electronically from the original observers, a digitizing scanner was used (a Hewlett Packard Scan Jet Plus hooked to a Macintosh SE). Once the scanned data were converted into a digital file (using the DATASCAN software package), this file was compared with the original image. Small (a few %) differences in both coordinate scales were often detectable. The scanner data were, therefore, "rectified" (i.e. transformed to the original axes) by assuming that slight axis tilts relative to the scanning frame had caused these minor differences (or nonlinearities in the reproduction of the original spectra). The digitized data were forced to match the original, with due regard to the linear, semi-logarithmic, or logarithmic character of the two axes, and with slightly different treatment according to whether the original spectrum was monotonic, or possessed strong sharp emission features. We found that the accurate representation of the latter required a slightly different rectification algorithm to that optimal for purely continuum spectra or those with broad absorptions. An interactive graphics routine was written (in the ANA language) to perform the rectification. The same routine converted ordinate scales into F_λ (in $\text{W cm}^{-2} \mu\text{m}^{-1}$) and all abscissae into wavelength (in μm), coping with any combination of linear and logarithmic coordinates, and any of F_λ , F_ν , λF_λ , $\lambda^3 F_\lambda$, νF_ν for the ordinate, and wavelength, wavenumber, or frequency for the abscissa.

Some spectra were obtained from original sources in digital form, namely: the collection of absolutely calibrated 1-5.5 μm spectra by Strecker, Erickson, and Witteborn (1979); and unpublished airborne spectra between ~ 16 and 65 μm of bright sources secured by Dr. Bill Glaccum as

part of his Ph.D. research.

Drs. Fred Witteborn and Jesse Bregman very kindly made available the copious databases at NASA-Ames of ground-based circular variable filter (sequential) spectra between 1 and 5.5 μm , and many airborne linear array (multiplex) spectra between 4 and 8 μm . These included unpublished 1.2-5.5 μm spectra of K and M giants, and 4-8 μm spectra of carbon stars taken at Mt Lemmon by Dr. Bregman. Dr. Don Strecker kindly supplied his unpublished archive of combined ground-based and airborne spectra (from which Strecker et al. 1979 was culled) in original form to be scanned.

b) Scaling and merging of spectra

Some spectra are published in absolute units; others appear only with relative ordinates. Regardless of which situation obtains, the absolute scaling of a fragment is achieved by direct comparison with photometry from the literature, converted into monochromatic spectral flux densities, and plotted over the spectrum (again using interactive graphics).

By this means, spectral fragments can be scaled at least relative to one another, whether they overlap or not. The routines devised involve matching of F_{λ} levels and gradients ($dF_{\lambda}/d\lambda$) of fragments in adjacent spectral bands, with simultaneous matching of each fragment to the available photometry. (In what follows, all procedures were carried out using interactive graphics routines written in ANA.) Even in the complete absence of photometry in some region (typically the 4-8 μm band), overlapping and matching of adjacent fragments should result in a valid spectral shape (i.e. relative calibration of fragments to one another). IRAS photometry also assisted in the scaling of spectra; the flux densities from the Point Source Catalog version 2 (1988: hereafter PSC2) were converted into F_{λ} using standard filter bandwidths (cf. IRAS Explanatory Supplement 1988, page X-13), color-corrected appropriately for the source under consideration (cf. IRAS Explanatory Supplement 1988, page VI-27), then turned to F_{λ} .

After achieving the best matches of fragments to each other and to the photometric points, the final spectrum was represented in regions of overlap by the data judged to have the best signal-to-noise after due consideration of atmospheric transmission. For some sources, the existing fragments in our database permitted the creation of a complete spectrum from 2-35 μm . This was then regridded to a uniform wavelength scale with step 0.1 μm at all wavelengths by linear interpolation to provide the final spectrum of each such source. This wavelength step is somewhat coarse for the 1-5 μm region and degrades the original spectral resolution; it is well-matched to typical low-resolution KAO spectra from 5-8 μm , but it oversamples LRS and long wave KAO data. It, therefore, represents a compromise but one that adequately represents the wavelength scale of the features typically encountered, most of which are broad or very broad (e.g., CO fundamental and first overtone; silicate and SiC features; ice absorptions; steam bands). Steps of 0.1 μm also avoid severe degradation of the spectra of sources with emission lines, such as planetary nebulae and HII regions.

c) Interpolating and extrapolating spectra

Many sources lack spectral data in some region of the 2-35 μm spectrum. Typical ground-based near-infrared spectra cover the 2-4 μm region in two pieces: ~ 2.0 -2.5 and ~ 2.9 -4.0 μm with a gap from ~ 2.5 -2.9 μm due to terrestrial absorption by water and CO_2 .

Frequently, the entire 4/5-8 μm region is absent from the database because no-one has obtained a spectrum from NASA's Kuiper Airborne Observatory (KAO). Even given a KAO spectrum, there may still be a gap through the terrestrial CO_2 band at roughly 4.27-4.47 μm (cf. Strecker et al. 1979). The longest² wavelength data are scarce because they too depend upon observations from the KAO. Even if KAO data do exist these may cover only the 16-30 μm region, again necessitating extrapolation to 35 μm . Given only an IRAS LRS spectrum, one must extrapolate longward of 22.7 μm .

In all these situations, the approximation that involves fewest assumptions about the source is to use a blackbody to represent the unobserved piece of spectrum. At short (<8.0 μm) wavelengths, on relatively normal stars, we used blackbodies corresponding to the stellar effective temperature (cf. Ridgway et al. (1980) for K and M giants). For extreme AGB stars we used a combination of two separate blackbodies; one (the warmer) was matched to both the broadband photometry and the shortest LRS spectral data, the other (the cooler) was matched so that the sum of both blackbodies matched the longest LRS spectral data and photometry. Highly extreme AGB stars (those with the reddest [12]-[25] indices) may completely lack short wavelength photometry, or at least have no known [2.2]. For those we generated K from the AGB evolutionary models described in the Appendix of WCVWS which supply theoretical approximations for the spectral energy distributions of these highly evolved stars. Generally these energy distributions are so steep that a combination of photometry, an LRS spectrum, and a single blackbody suffices to represent these sources.

In some categories, where we had an incomplete series of fragments for one source, but a second source in the same category had complementary fragments to those of the first, we substituted the latter for the absent spectral fragment(s) of the first source. An example of this arises for the category AGB M 17 where GL 3022 has 2-4, 8-13 μm , and LRS data but X Her has only a KAO 16-40 μm fragment. These were combined to create "a complete spectrum" for GL 3022, the better represented source. This is justifiable because, even if both sources possessed complete spectra, they would have been averaged after normalization to provide a single template for the category.

When the longest wave data were completely absent we extrapolated using the best fitting (cool) blackbody to the LRS and/or 8-13 and/or 16-30 μm fragments. All such extrapolations were additionally guided by ground-based 18/20/22 or IRAS 25 μm photometry.

d) Variable stars

Many of the categories by their intrinsic nature are variable sources, namely the AGB stars. For these we attempted to select nearly contemporaneous photometry, or always to use the upper envelope of the variety of photometric points available at each wavelength. Of course, there are never sufficient spectra to match fragments to photometry at the appropriate phases in the cycles of these (typically Mira) variable stars. Indeed, we do not yet know whether the low resolution spectra longward of 8 μm of most of these extreme AGB stars (or even of the less extreme Miras with modest periods ~ 1 yr) vary with phase of the light curve.

However, it is encouraging that the 8-13 μm spectra for such stars in the literature based on observations in the 1970s overlap substantially with the much more recent IRAS LRS spectra. Such accords suggest that our method has not done violence to the spectra of many of

these sources.

To demonstrate the template technique and to show the effects of using a variable star, Fig. 1 presents the entire construction of the 2-35 μm spectrum for V Cyg.

e) Problems with "normal" stars

"Normal" stars can pose substantial difficulties in the infrared when complete spectra are sought, either for general templating or for the provision of absolute flux calibrators. Even if these stars (earlier than K) possessed LRS spectra, these usually decay so rapidly that the signal-to-noise ratios are unacceptably poor longward of $\sim 10 \mu\text{m}$. To provide spectra of the earlier type dwarf stars, we utilized the best-fitting blackbody to the combined LRS spectrum (noisy or not) and as complete a set of photometry as possible (including the IRAS points at 12 and 25 μm which often constituted the only photometry longward of 5 μm). This blackbody could be substituted for the absent spectral fragments both shortward and longward of the LRS range, and even for the entire (or any part of the) real LRS spectrum if this proved unacceptably noisy.

A further problem encountered in studying the LRS spectra of normal stars appears to arise from an inappropriate subtracted electronic baseline (IRAS Explanatory Supplement 1988, pages IX-11, X-41). This can produce an LRS spectrum that rapidly either tends to zero (too large a baseline removed) or climbs unphysically (too small a baseline removed) at long wavelengths. We dropped our potential template of ζ Oph for this reason ("B0.1 V") and substituted that of α Vir created by the photometry, LRS, and single blackbody method just described.

Finally, in the context of LRS spectra, we have "corrected" all LRS spectra used herein by the function tabulated by Volk and Cohen (1989a) to "dewarp" the spectra. We drew these spectra directly from the complete Dutch LRS database rather than working with the very restricted and incomplete LRS Atlas of Low Resolution Spectra (1986).

Note that we could not always locate a star/source with an adequate LRS spectrum of the precise spectral type required by some categories. In such cases, we used the closest match by type; e.g. δ Pav (G7 IV) to represent category "G5 V".

f) Exotic objects

For reflection nebulae, planetaries, and galaxies it was necessary to scale spectral fragments very carefully according to the apertures used in the original spectroscopy. These rescaled fragments were then compared with the largest aperture photometry or spectrophotometry available in the literature. For planetary nebulae, we checked both the levels of the near-infrared continuum and of emission line peaks to assure meaningful rescaling. Some planetaries lack any fragmentary spectra shortward of $\sim 3.0 \mu\text{m}$, although broadband photometry exists. For these we extrapolated shortward of $\sim 3.0 \mu\text{m}$ using an optically thin free-free continuum (essentially $F_\lambda \propto \lambda^{-2}$ since the total wavelength range for extrapolation was so small that variations in the Gaunt factor were negligible). We approximated our initial estimate of infrared continuum on the basis of known radio continuum flux and extinction, but rescaled the free-free continuum level on the basis of comparison with near-infrared photometry.

For some of the more extreme AGB M stars we could not locate short wavelength fragments, although both photometry and LRS spectra exist. Many

of these are known as OH/IR stars, with OH and GL (Price and Murdock 1983) designations. Hyland et al. (1972) and Gehrz et al. (1985) provide useful photometry that defines the overall spectral energy distributions of these OH/IR sources.

The most extreme AGB C stars and the AGB CI objects have no known optical counterparts and near-infrared photometry is lacking. The reddest [12]-[25] indices we could find for the former were 1.00 (TT Cen) and 1.88 (HD 100764). We, therefore, linearly interpolated in both [12]-[25] and [2.2]-[12] between these two stars to obtain generic "photometry" for the intervening categories (AGB C 13, 15, 17). These latter categories were then treated by the method involving photometry, an LRS spectrum (defined as the average of the spectra of many IRAS sources with the desired [12]-[25] indices: cf. WCVWS), and a single blackbody (as described above for normal stars).

g) Template generation: correction for interstellar reddening

Once the complete spectra for all the individual sources had been created we converted these into templates as follows. First, the literature was consulted to provide an estimate of the purely interstellar component of extinction. For all the AGB stars, we assumed that the dominant source of extinction was circumstellar and therefore represented the intrinsic character of the star. No dereddening was attempted for these. Second, the individual spectra were checked for artefacts of the interpolation, regridding, and splicing procedures (such as discontinuities in level or slope, or inappropriately elevated sections within an otherwise locally flat spectrum). Appreciable artefacts were removed by recreating the entire template more carefully; modest artefacts by local blackbody interpolation; small ones were ignored because subsequent smoothing of the spectra would handle them adequately. Third, any long wavelength substitutions by blackbodies were reexamined for improved matches with photometry and spectral fragments using a reddened blackbody suffering the same extinction as determined for the source. Fourth, the spectra were dereddened (the law is described below). Finally, the intrinsic spectra were smoothed using Gaussians; typically, light smoothing (FWHM of $0.5 \mu\text{m}$) was useful between 2 and $10 \mu\text{m}$; beyond $\sim 15 \mu\text{m}$, the FWHM was increased, usually to 1.0 (sometimes 1.5) μm . In each case, the region(s) over which the smoothing was applied and the specific degree(s) of smoothing were chosen to suit the individual spectrum; it could be as little as a few spectral grid points or as large as the entire spectral range (minus the obligatory few endpoints where no smoothing was applied by the algorithm). Many spectra of bright sources required no smoothing at all or only over very restricted wavelength ranges (to cope with slight residual problems with the splicing of fragments in regions of overlap).

The law of interstellar extinction was extended from that used by WCVWS by applying a $1/\lambda$ extrapolation beyond $22.7 \mu\text{m}$ (the end of the LRS range) and a van der Hulst #15 law shortward of $7.67 \mu\text{m}$. Fig. 2 presents the complete function, A_λ/A_v .

Finally, we combined the smoothed intrinsic templates for each category represented by more than a single source. A simple average was used in almost all cases unless the simultaneous display of all the individual source templates indicated that any one was unusual or distinct from all the others (differing either in energy distribution or in the length of the unobserved sections of spectrum). Such spectra were omitted from the average (and are indicated by source names in {} in Table 1).

Exceptions to the averaging process were T Tau Stars and Planetary Nebulae. The former were represented by (4 * AB Aur + 2 * RY Tau + 2 * GW Ori + HL Tau + R Mon) to achieve the presence of silicate emission in 80% and of absorption in 20% of the class (Cohen and Witteborn 1985), and to utilize the unpublished KAO spectrum for HL Tau.

We note that WCVWS divided planetaries into "blue" and "red" subtypes, depending on their [12]-[25] color index. Volk and Cohen (1990) recently summarized the LRS spectra for 170 planetaries from which one can derive the frequencies of occurrence of the distinct archetypal LRS spectral shapes. We first assume that group "F" nebulae, which have very noisy spectra, would all be placed within the remaining seven groups with the same frequencies as the bulk of the population display, if the LRS spectra were less noisy. Then we treat planetaries as occurring with seven archetypal LRS shapes which are found with the following frequencies (%): D, 7.6; R, 31.0; P, 15.2; L, 6.3; H, 28.5; X, 2.6; E, 8.8 (the reader is referred to Volk and Cohen for an explanation of the letter designations). Spectra are available from the literature for only 3 "Blue Planetary Nebulae", namely GL 618 (group D), BD+30°3639 and M2-56 (both in group P). Group P nebulae are twice as common as group D so the simple average of the spectra of these 3 nebulae faithfully represents the relative populations of blue planetaries. We take this average to represent the "PN BLUE" category. Red planetaries span all 7 LRS shapes. We, therefore, require a template for each archetype. A search of the spectra available and of the wider literature suggested the following choices: group D, NGC 6572; R, IC 4997; P, IC 418 and NGC 7027; L, He 2-131; H, Hb 5 and IC 2621; X, NGC 6302; E, NGC 7026. Consequently, we represent the "PN RED" category by the following linear combination of spectral templates: $0.076 \cdot \text{NGC 6572} + 0.31 \cdot \text{IC 4997} + 0.076 \cdot \text{NGC 7027} + 0.076 \cdot \text{IC 418} + 0.063 \cdot \text{He 2-131} + 0.143 \cdot \text{Hb 5} + 0.143 \cdot \text{IC 2621} + 0.026 \cdot \text{NGC 6302} + 0.088 \cdot \text{NGC 7026}$.

To define the spectra for IC 4997 and NGC 7026 for which no spectral fragments outside the LRS range could be found, we first used the two-blackbody method (described above for extreme AGB stars) to fit the photometry and LRS, then modified the near-infrared continua to follow a free-free slope based on their radio continuum fluxes.

All these procedures resulted in the creation of 88 separate templates (87 Galactic; and a single one resulting from the combination of all three galaxy spectra). Fig. 3 presents 6 of these templates.

h) Extragalactic templates

In general, galaxies play only a minor role in our Model unless we consider long wavelengths (25 μm), very low flux levels, and high galactic latitudes (cf. WCVWS). Consequently, only 4 types of galaxy are required by the Model ("blue normal" and "red normal" galaxies, Seyferts, and quasars). WCVWS chose to adopt the same LRS spectral signature for all galaxies (essentially the average found by Cohen and Volk (1989) in their search of the complete LRS database for known galaxies), but they tilted this LRS spectrum to match the different [12]-[25] indices for these 4 types of galaxy. Although not strictly accurate (only 31% of "active galaxies" - Seyferts of types 1 and 2, LINERS, or quasars - have the emission bands; the remaining 69% present power law spectra; Aitken and Roche 1985; Roche et al. 1984), this suffices for our purposes (because the Model includes the effects of cosmology but not yet of evolution).

For the new version of the Model, we derive our basic galaxy template as the average of those for M82, NGC 1068, and NGC 253. This is

then tilted appropriately to yield separate templates for the 4 extragalactic categories.

i) Filling in unobserved photospheric features

The averaged intrinsic templates finally require treatment to cope with regions of the spectrum that have not been observed. If, for example, a category is represented by 3 separate sources for only one of which there exists a 5-8 μm airborne spectrum, we spliced this portion of the smoothed template of that particular source back into the average template for the category, with correct normalization to fit the adjacent spectrum.

Often we lacked the 2.5-2.9 and 4.0-5.2 μm portions of a spectrum. The former includes the first overtone of CO in cool stars, the latter the CO fundamental near 4.7 μm . However, Arnaud et al. (1989) have published low-resolution 2.0-2.5 μm spectra for a wealth of cool stars, of both dwarf and giant luminosity. We incorporated these first overtone fragments, suitably normalized to overlap the adjoining continua, into our final average templates. In general, we were able to use a fragment corresponding to the same spectral type as the template represented.

For the CO fundamental, far fewer spectra exist. A number exist in the unpublished archive assembled by Strecker. Dr. Jesse Bregman provided a very useful set of unpublished spectra (sequentially obtained, wavelength by wavelength) from a 1977 October run at the NASA 1.5 m Mt Lemmon telescope. These represent contemporaneous measurements in the 1.2-2.4, 3.0-4.2, and 4.4-5.6 μm windows of a number of K and M giants (α Aur G5 III+G0 III; δ And K3 III; α Tau K5 III; 2 Peg M1 III; HR 8621 M4 III; EU Del M6 III; TX Cam M10; U Ori OH/IR Mira). These constitute the basis for an incomplete but extremely valuable set of normalized fragments spanning the CO fundamental. We were able to supply the CO fundamental region for missing spectral types by averaging adjacent ones (e.g. the normalized average of M4 III and M6 III spectra was used to represent that for an M5 III, etc.).

It has been possible to accommodate very recently obtained new airborne spectra of relevant types, too. For example, a 2.4-8.0 μm high-resolution spectrum of the extreme AGB M GL 1686 was acquired in 1990 April (using both Dr. Bregman's and Dr. Witteborn's instruments during a deployment the KAO in New Zealand to observe Supernova 1987A). This showed a complete absence of any CO fundamental, perhaps due to shrouding by circumstellar dust emission. This, therefore, provides support for a smooth featureless interpolation across the 4.7 μm region in other (and more) extreme AGB M stars. Likewise, featureless interpolations were justified in extreme carbon stars by the generally blackbodylike nature of their infrared continua in which even the 3.1 μm polyatomic feature is absent or very weak. We used the unpublished 4-8 μm KAO spectrum of UU Aur (AGB C 03: see Table 2) to represent this unobserved region in R Lep (AGB C 03) and S Cep (AGB C 05). Other new KAO spectra that proved valuable were 5-8 μm spectra of R LMi and α Her taken in 1990 April. R LMi would be categorized as an AGB M 07 so we applied its KAO fragment to the spectra of TX Cam and RS Cnc (AGB M 05) after suitable multiplicative rescaling. α Her was substituted for the "M3-4 I-II" Model category.

j) "Missing" categories

Even with such a large database of spectra, some categories were still not represented, usually because of their rarity. For the extreme AGB

M types, AGB M 21 and 25, only OH/IR stars with no spectra or only a near-infrared fragment could be found. It was, therefore, deemed more accurate to represent AGB M 21 by the average of the two adjacent categories (M 19 and 23) for which good spectral coverage was obtained than to extrapolate using the photometry and LRS fragment alone. AGB C categories 13, 15, and 17 were generated from the Model's average LRS spectra for these categories (WCVWS) and the photometry created by interpolating [2.2]-[12] and [12]-[25] (discussed in IIIf). AGB C types 21, 23, and 25 were taken to have the same template as that for AGB C 19 as did WCVWS. In the intervening year, no example of a confirmed extreme AGB C star has been discovered with [12]-[25]>2.00, in spite of several concerted and systematic attacks on the complete LRS database (Volk and Cohen 1989b; Volk et al. 1990a,b). Likewise, no sources have been uncovered to represent the AGB CI categories with [12]-[25]>2.00 so that we take the spectrum for type AGB CI 19 to represent all the categories from AGB CI 21 to 31. AGB CI 11 is taken as the average of CI types 09 and 13.

IV. OTHER CHANGES IN THE NEW MODEL

The details of the actual code used to calculate the densities and brightnesses of sources along the direction of integration were maintained exactly as described by WCVWS. Further, we have introduced no changes in the source tables for M_{12} and M_{25} . Therefore, the many mid-infrared validations of the previous Model described (and in some cases displayed explicitly) by WCVWS still pertain to the new Model.

a) Surface brightness algorithm

Two modifications were introduced. First, an additional algorithm was incorporated to calculate the cumulative surface brightness from the differential (Log N, Log S) table for each level of flux or magnitude desired. This corresponds simply to smearing the point sources observed over the area sampled and has its output in Watts $m^{-2} deg^{-2}$. These brightnesses may be compared directly with the maps of the Galactic Plane at 2.4 and 3.4 μm summarized by Okuda (1981) in his Table I. The new Model does not detect greater fluxes in its point source calculations than are inherent in these near-infrared surveys and hence does not violate any constraints imposed by these. However, such comparisons do not strictly constitute a validation of the new Model for the Model deals strictly with the content of the point source sky while the rocket and balloon experiments near 2.4 μm utilize large beams, sensitive to diffuse radiation as well as point sources.

b) Absolute near-infrared magnitudes

WCVWS were primarily concerned with the LRS spectral range. Consequently, although they were able to demonstrate reasonable matches of their Model to 2 μm source counts, their inherent source table of absolute K magnitudes (M_K) could not always be validated by reference to explicit spectra or to the literature. While there are still categories unobserved spectroscopically within the realm of the present version of our Model, there are complete spectral representations. We, therefore, were able to examine the M_K table in greater detail than did WCVWS. In particular, we convolved the system efficiency profiles of the IRAS band 1 and 2 filters (12 and 25 μm) and that for the original Johnson (1965: his

Appendix table A-2) K filter with each of the 87 Galactic templates (with appropriate allowance for the extrapolation of our spectra below $2.0 \mu\text{m}$ to accommodate the continuation of the K filter shortward of $2.0 \mu\text{m}$). We then compared the M_K that resulted by constraining M_{12} (and M_{25}) to match the tables of WCVWS, with those derived from the values of intrinsic K-[12] that could be gleaned from the literature on the individual sources generating our templates. These two sets of M_K were combined to create a new set of tables for M_K , M_V , M_J , M_H , and $M_{2.4}$ that differ somewhat from those used by WCVWS. Similarly, we created a Gaussian filter profile to represent the Japanese experiments at $2.4 \mu\text{m}$, with effective wavelength $2.38 \mu\text{m}$ and FWHM $0.09 \mu\text{m}$ (cf. Hayakawa et al. 1981; Maihara et al. 1978). Convolution of this Gaussian with the 87 templates created a new table for $M_{2.4}$.

In essence, while the new absolute magnitude tables differ from the old, their effects on luminosity functions are minimal. Following WCVWS we recreated the V and K luminosity functions and found them virtually indistinguishable from those presented by WCVWS. This similarity results from the fact that the principal alterations in absolute magnitudes are for those categories with very red spectra and very low population densities. However, we prefer the new tables because they represent consistency between the two modes of application of the Model; i.e. one now achieves basically identical predicted source counts whether using the "hard-wired" K and [2.4] filters or using the "customized" version in which an arbitrary filter profile may be entered and carried through the modeling. (This consistency at short wavelengths was not required in the work of WCVWS where custom filters had to fall wholly within the LRS spectral range.)

V. VALIDATIONS OF THE NEW MODEL

For meaningful comparisons with direct observations we confine our attention to point source surveys. The wavelength at which most source counts relevant to the new Model have been carried out is $2.2 \mu\text{m}$. We have, therefore, compared the predictions of the new Model at K with the north Galactic polar counts of Elias (1978); source counts in all 7 zones in the Galactic plane by Eaton, Adams, and Giles (1984); and all 4 of the 6 zones in the plane measured by Kawara et al. (1982) that represent contiguous areas. (Note that the set of counts by Eaton, Adams, and Giles were converted to cumulative count per square degree while those by Kawara et al. represent cumulative counts for each total zone, and zone areas vary between 3.2 and 48.0 square degrees.) Figs. 4-6 present these 12 comparisons.

The Model does as well as the version by WCVWS in the Eaton et al. regions, that is, it matches very well except near $l=29^\circ$, where it falls short of reality by a factor of 2 at the brightest magnitudes, and at the Center, where the bulge stars are overpredicted by a factor of 2. The comparisons with the Kawara et al. counts show essentially the same phenomenon: agreement well within a factor of 2 except for $l=26-28^\circ$. The discrepancies could arise either because our representation of the molecular ring is too simplistic, or because the extinction is treated too simply (i.e. uniformly with distance) by our Model. At the north Galactic pole, the agreement with Elias's counts is excellent.

We conclude that such these counts do not indicate any major discrepancies (greater than a factor of ~ 2) between the Model's predictions and actual counts.

VI. CONCLUSIONS

The newest version of the Point Source Infrared Sky Model performs identically to its earliest version at 12 and 25 μm , and at least as well at 2.2 μm . It will now accommodate all filters whose transmission curves extend from zero to zero wholly within the 2.0 to 35.0 μm range, with consistency between tables of broadband absolute magnitudes and those derived by integration of actual filter/system efficiency profiles over the real spectra. It can also yield estimates of the surface brightness of the point sources smeared across the desired area, as a function of threshold sensitivity.

The library of spectra used to generate the complete templates for the new Model is capable of providing calibration spectra for future infrared missions both because some of the relevant calibration sources have been examined spectroscopically, and because one can apply the generic templates to all sources for which there exist categorizations as used in the Model.

VII. REFERENCES

- Aitken, D. K., and Roche, P. F. 1982, M.N.R.A.S., 200, 217.
 Aitken, D. K., and Roche, P. F. 1985, M.N.R.A.S., 213, 777.
 Aitken, D. K., Roche, P. F., and Allen, D. A. 1982, M.N.R.A.S., 200, 6P.
 Arnaud, K. A., Gilmore, G., and Collier-Cameron, A. 1989, M.N.R.A.S., 237, 495.
 Ashley, M. C. B., and Hyland, A. R. 1988, Ap.J., 331, 532.
 Berriman, G., and Reid, N. 1987, MNRAS, 227, 315.
 Cohen, M. 1975, M.N.R.A.S., 173, 279.
 Cohen, M. 1980, M.N.R.A.S., 191, 499.
 Cohen, M. 1984, M.N.R.A.S., 206, 137.
 Cohen, M., Allamandola, L. J., Tielens, A.G.G.M., Bregman, J., Simpson, J. P., Witteborn, F. C., Wooden, D., and Rank, D. 1986, Ap.J., 302, 737.
 Cohen, M., Tielens, A. G. G. M., Bregman, J. D., Witteborn, F. C., Rank, D. M., Allamandola, L. J., Wooden, D. H., and de Muizon, M. 1989, Ap.J., 341, 246.
 Cohen, M., and Volk, K. 1989, A.J., 98, 1563.
 Cohen, M., Wainscoat, R. J., Walker, R. G., Volk, K., Walker, H. J., and Schwartz, D. E. 1990, NASA, CR 177526.
 Cohen, M., and Witteborn, F. C. 1985, Ap.J., 294, 345.
 Cutri, R. M. et al. 1981, Ap.J., 245, 818.
 Eaton, N., Adams, D. J., and Giles, A. B. 1984, M.N.R.A.S., 208, 241.
 Eiroa, C., Hefele, H., and Zhang-Yu, Q. 1983, A.A.Suppl, 54, 309.
 Eiroa, C., Neckel, Th., Sanchez Magro, C., and Selby, M. J. 1981, A.A., 95, 206.
 Elias, J. H. 1978, A.J., 83, 791.
 Engelke, C. W. 1990, Report on "LWIR Stellar Calibration", Lincoln Laboratory, M.I.T.
 Forrest, W. J., et al. 1978, Ap.J., 219, 114.
 Forrest, W. J., McCarthy, J. F., and Houck, J. R. 1979, Ap.J., 233, 611.
 Forrest, W. J., Houck, J. R., and McCarthy, J. F. 1981, Ap.J., 248, 195.
 Gehrz, R. D., Kleinmann, S. G., Mason, S., Hackwell, J. A., and Grasdalen, G. L. 1985, Ap.J., 290, 296.

- Giguere, P. T., Woolf, N. J., and Webber, J. C. 1976, *Ap.J. (Letters)*, 207, L195.
- Glaccum, W. 1990, Ph.D. dissertation.
- Goebel, J. H., Bregman, J. D., Strecker, D. W., Witteborn, F. C., and Erickson, E. F. 1978, *Ap.J. (Letters)*, 222, L129.
- Goebel, J. H., and Moseley, S. H. 1985, *Ap.J. (Letters)*, 290, L35.
- Hacking, P., and Houck, J. R. 1987, *Ap.J. Suppl.*, 63, 311.
- Hayakawa, S., Matsumoto, T., Murakami, H., Uyama, K., Thomas, J. A., and Yamigami, T. 1981, *A.A.*, 100, 116.
- Houck, J. R., Forrest, W. J., and McCarthy, J. F. 1980, *Ap.J. (Letters)*, 242, 265.
- Houck, J. R., Shure, M. A., Gull, G. E., and Herter, T. 1984, *Ap.J. (Letters)*, 287, L11.
- Hyland, A. R., Becklin, E. E., Frogel, J. A., and Neugebauer, G. 1972, *A.A.*, 16, 204.
- IRAS Catalogs and Atlases, Vol. 1, Explanatory Supplement. 1988, eds. C. A. Beichman, G. Neugebauer, H. Habing, P. E. Clegg, and T. J. Chester (Washington, DC: GPO).
- IRAS Catalogs and Atlases, Vols. 2-6, The Point Source Catalog. 1988, eds. C. A. Beichman, G. Neugebauer, H. Habing, P. E. Clegg, and T. J. Chester (Washington, DC: GPO).
- IRAS Catalogs and Atlases, Atlas of Low Resolution Spectra, 1986, IRAS Science Team, *A. A. Suppl.*, 65, 607.
- Isaacman, R. 1984, *A.A.*, 130, 151.
- Johnson, H. L. 1965, *Ap.J.*, 141, 923.
- Jones, B., Merrill, K. M., Puetter, C. R., and Willner, S. P. 1978, *A.J.*, 83, 1437.
- Jones, T. J., Hyland, A. R., Fix, J. D., and Cobb, M. L. 1988, *A.J.*, 95, 158.
- Kawara, K., Kozasa, T., Sato, S., Kobayashi, Y., Okuda, H., and Jugaku, J. 1982, *Publ. A. S. Japan*, 34, 389.
- Knacke, R. F., Puetter, R. C., Erickson, E. F., and McCorkle, S. 1985, *A.J.*, 90, 1828.
- Magazzu, A., and Strazzulla, G. 1989, in *Proc. 22nd ESLAB Symposium, "Infrared Spectroscopy in Astronomy"*, ed. B. H. Kaldeich, ESA SP-290, p.371.
- Maihara, T., Oda, N., Sugiyama, T., and Okuda, H. 1978, *Publ. A. S. Japan*, 30, 1.
- McCarthy, J. F., Forrest, W. J., and Houck, J. R. 1978, *Ap.J.*, 224, 109.
- Merrill, K. M., and Stein, W. A. 1976a, *P.A.S.P.*, 88, 285.
- Merrill, K. M., and Stein, W. A. 1976b, *P.A.S.P.*, 88, 294.
- Merrill, K. M., and Stein, W. A. 1976c, *P.A.S.P.*, 88, 874.
- Noguchi, K., Maihara, T., Okuda, H., Sato, S., and Mukai, T. 1977, *P.A.S. Japan*, 29, 511.
- Okuda, H. 1981, in *IAU Symp. No. 96, "Infrared Astronomy"*, eds. C. G. Wynn-Williams and D. P. Cruikshank (D. Reidel: Holland), p.247.
- Price, S. D., and Murdock, T. L. 1983, "The Revised AFGL Infrared Sky Catalog", *AFGL-TR-83-0161*, ADA134007.
- Puetter, R. C., Russell, R. W., Sellgren, K., and Soifer, B. T. 1977, *P.A.S. Pacific*, 89, 320.
- Ridgway, S. T., Joyce, R. R., White, N. M., and Wing, R. F. 1980, *Ap.J.*, 235, 126.
- Roche, P. F., and Aitken, D. K. 1986, *M.N.R.A.S.*, 221, 63.
- Roche, P. F., Aitken, D. K., Phillips, M. M., and Whitmore, B. 1984,

- M.N.R.A.S., 207, 35.
- Russell, R. W., Soifer, B. T., and Merrill, K. M. 1977, Ap.J., 213, 66.
- Russell, R. W., Soifer, B. T., and Willner, S. P. 1977, Ap.J. (Letters), 220, L49.
- Russell, R. W., Soifer, B. T., and Willner, S. P. 1978, Ap.J., 220, 568.
- Scargle, J., and Strecker, D. W. 1979, Ap.J., 228, 838.
- Sellgren, K. 1986, Ap.J., 305, 399.
- Sellgren, K., Allamandola, L. J., Bregman, J., D., Werner, M. W., and Wooden, D. H. 1985, Ap.J., 299, 416.
- Strecker, D. W., Erickson, E. F., and Witteborn, F. C. 1978, A.J., 83, 26.
- Strecker, D. W., Erickson, E. F., and Witteborn, F. C. 1979, Ap.J. Suppl., 41, 501.
- Volk, K., and Cohen, M. 1989a, A.J., 98, 1918.
- Volk, K., and Cohen, M. 1989b, A.J., 98, 931.
- Volk, K., and Cohen, M. 1990, A.J., 100, 485.
- Volk, K., Stencel, R. E., Brugel, E. W., and Kwok, S. 1990a, "Supplementary IRAS LRS Spectra of 842 Sources Brighter than 20 Jy not Included in the LRS Atlas", preprint.
- Volk, K., Stencel, R. E., Brugel, E. W., and Kwok, S. 1990b, "Supplementary IRAS LRS Spectra of 1810 Sources Brighter than 10 Jy not Included in the LRS Atlas", preprint.
- Wainscoat, R. J., Cohen, M., Volk, K., Walker, H. J., and Schwartz, D. E. 1990, in preparation (WCVWS).
- Walker, R. G., and Cohen, M. 1989, Contractor's Final Report to Boeing Aerospace (CZ 1521).
- Willner, S. P. et al. 1982, Ap.J., 253, 174.
- Willner, S. P., Jones, B., Puetter, R. C., Russell, R. W., and Soifer, B. T. 1979, Ap.J., 234, 496.
- Willner, S. P., Soifer, B. T., Russell, R. W., Joyce, R. R., and Gillett, F. C. 1977, Ap.J. (Letters), 217, L121.
- Witteborn, F. C., Strecker, D. W., Erickson, E. F., Smith, S. M., Goebel, J. H., and Taylor, B. J. 1980, Ap.J., 238, 577.

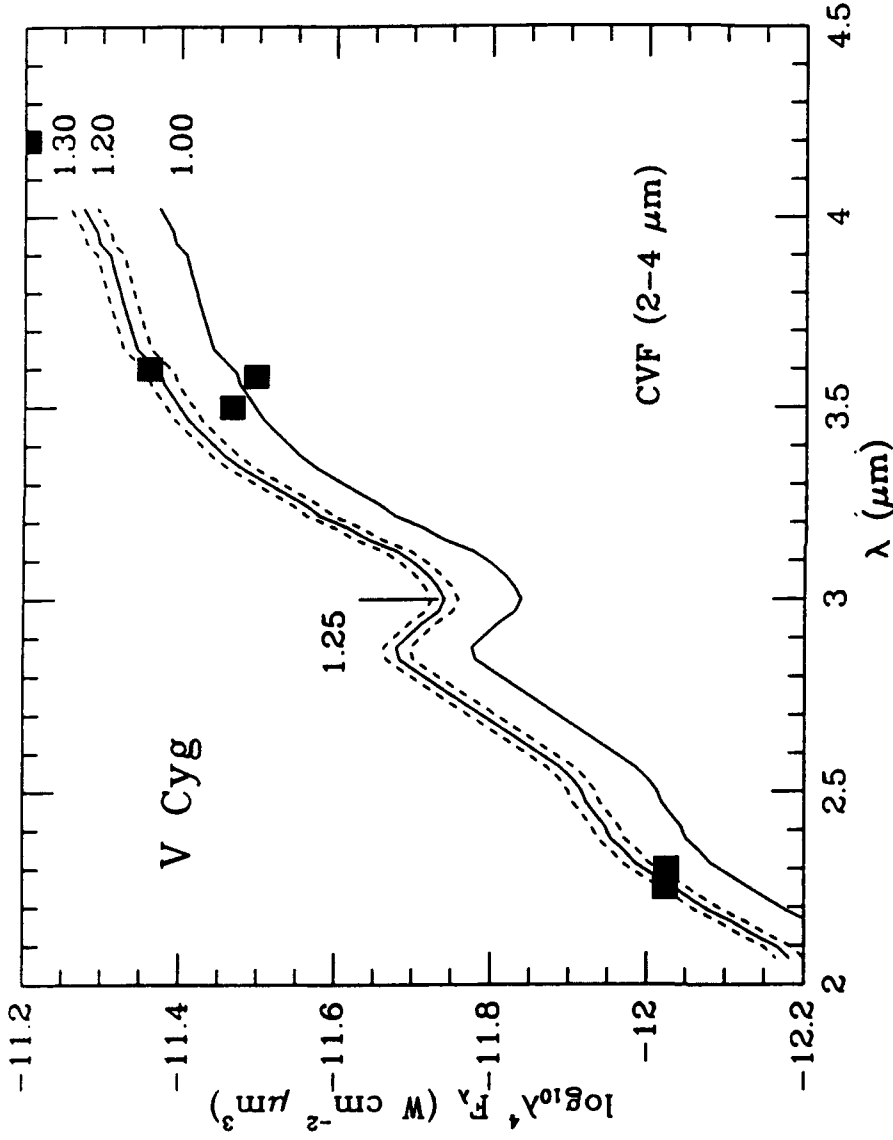


Fig. 1: Sequence of displays representing the construction of the complete 2-35 μm template for the variable V Cyg. Plots are $\log \lambda F_{\lambda}$ vs. λ to compress the displays for steeply falling spectra (essentially to remove the longer wavelength Rayleigh-Jeans fall-off in normal stars).

Fig. 1: a) ground-based CVF data with nominal scaling (1.00 curve) and best match (solid, 1.25) fit to the broadband photometry (filled squares) showing plausible range of scale factors (1.20-1.30) that might also be fit to the photometry. The fitting is designed to favor the upper envelope of the photometry (so that one might renormalize all fragments to the maximum of the star).

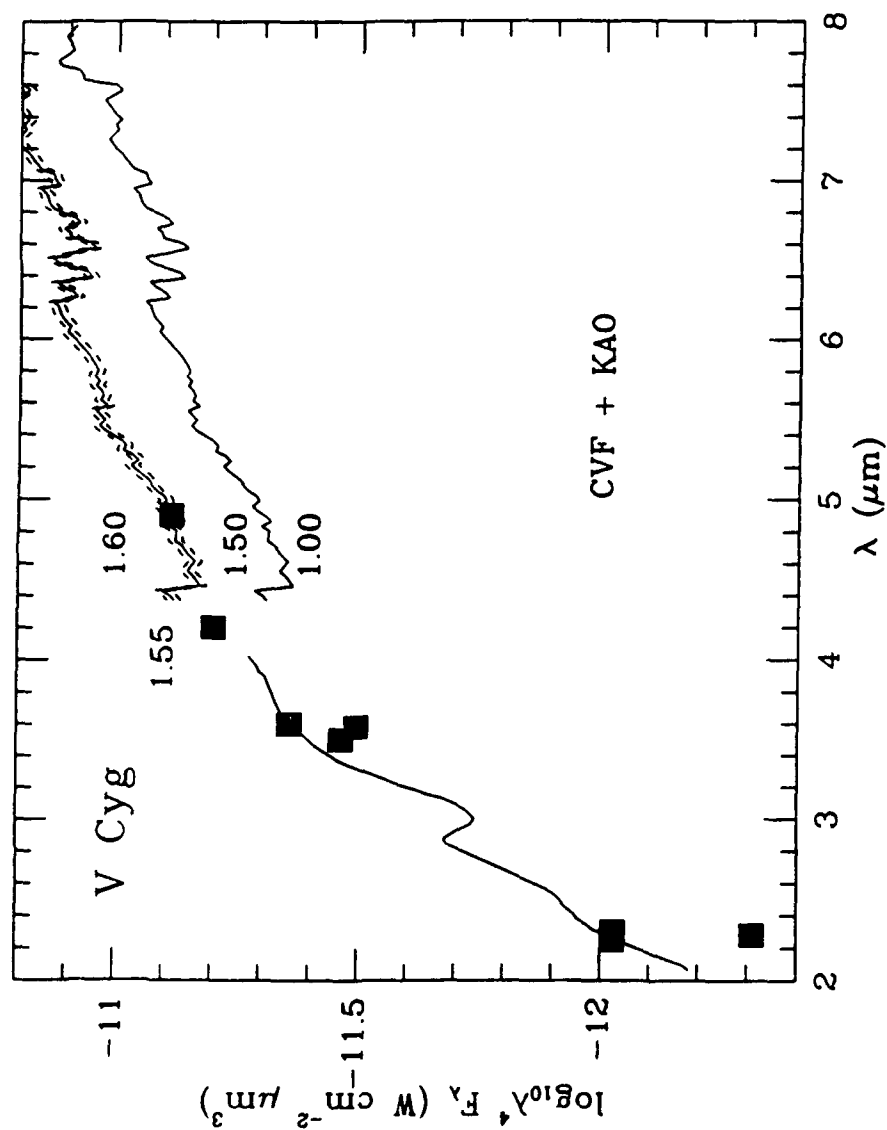


Fig. 1: b) matching the CVF and KAO spectra; again, 1.00 represents the curve scanned in the literature which required scaling up by 1.55 (in the range 1.50-1.60 plausibly) to fit both the photometry at 4.2 and 4.9 μm and the already scaled CVF fragment.

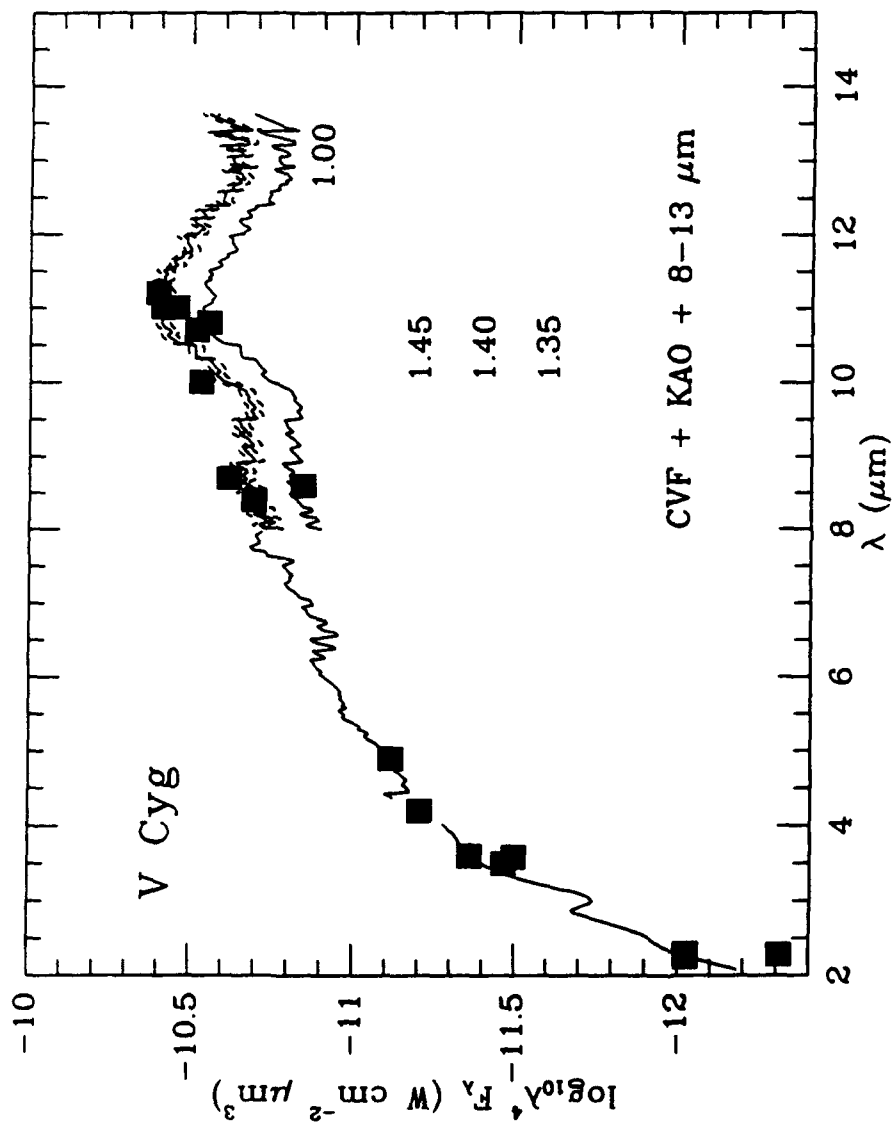


Fig. 1: c) merging CVF+KAO with the 8-13 μm spectrum from the literature. Note that the rescaling again favors the upper envelope of the photometry.

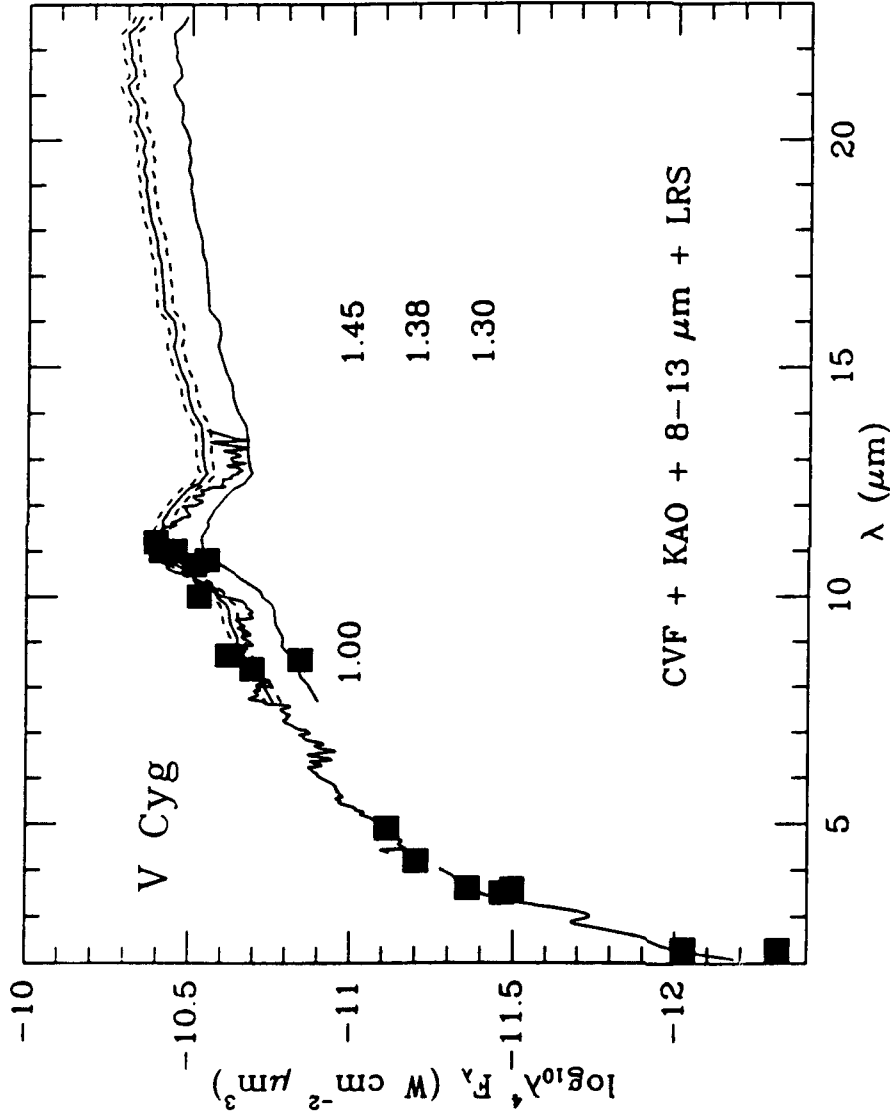


Fig. 1: d) merging CVF+KAO+8-13 μm with the IRAS LRS spectrum. The finally adopted best-fit involved rescaling by a factor 1.38 over the nominal calibrated average LRS spectrum; the plausible range of this factor is 1.30-1.45 (as represented by the two dashed curves that flank the selected best fit).

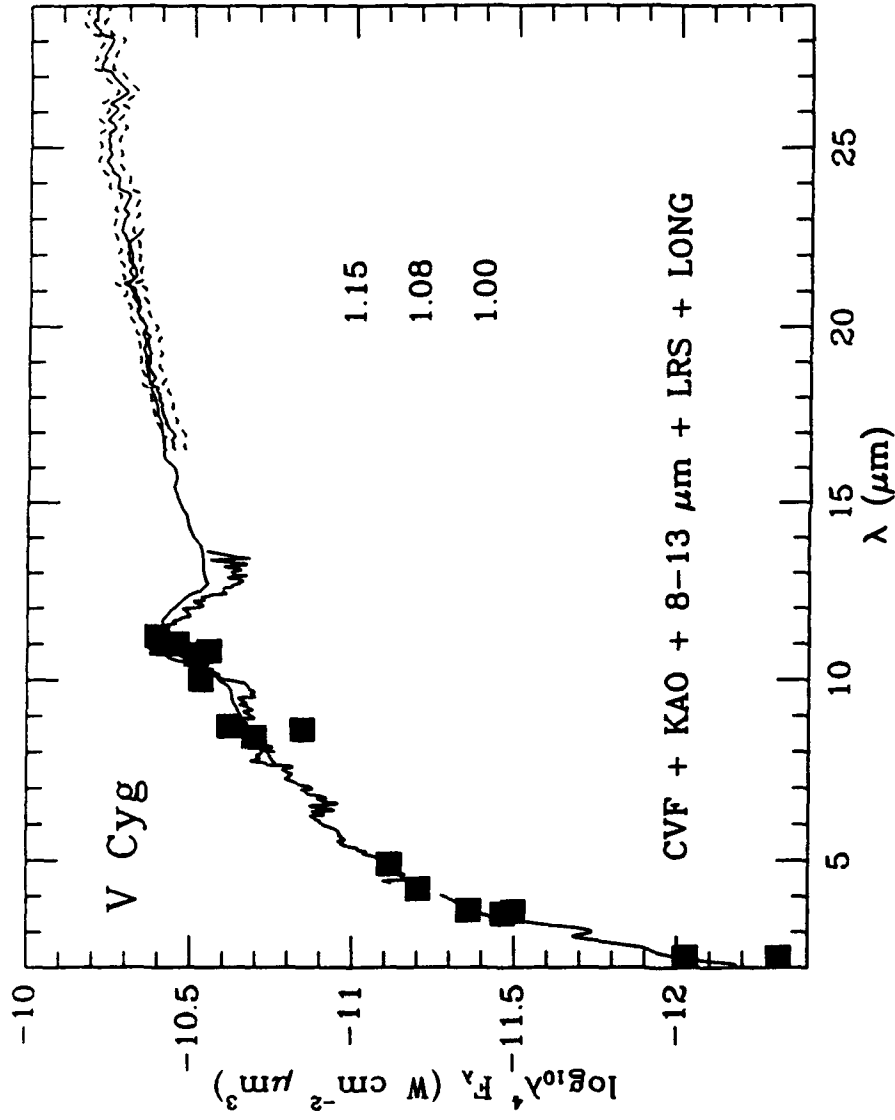


Fig. 1: e) further merging with the long wavelength KAO spectrum (from ~ 16 -30 μm). Best fit factor=1.08, range 1.00-1.15.

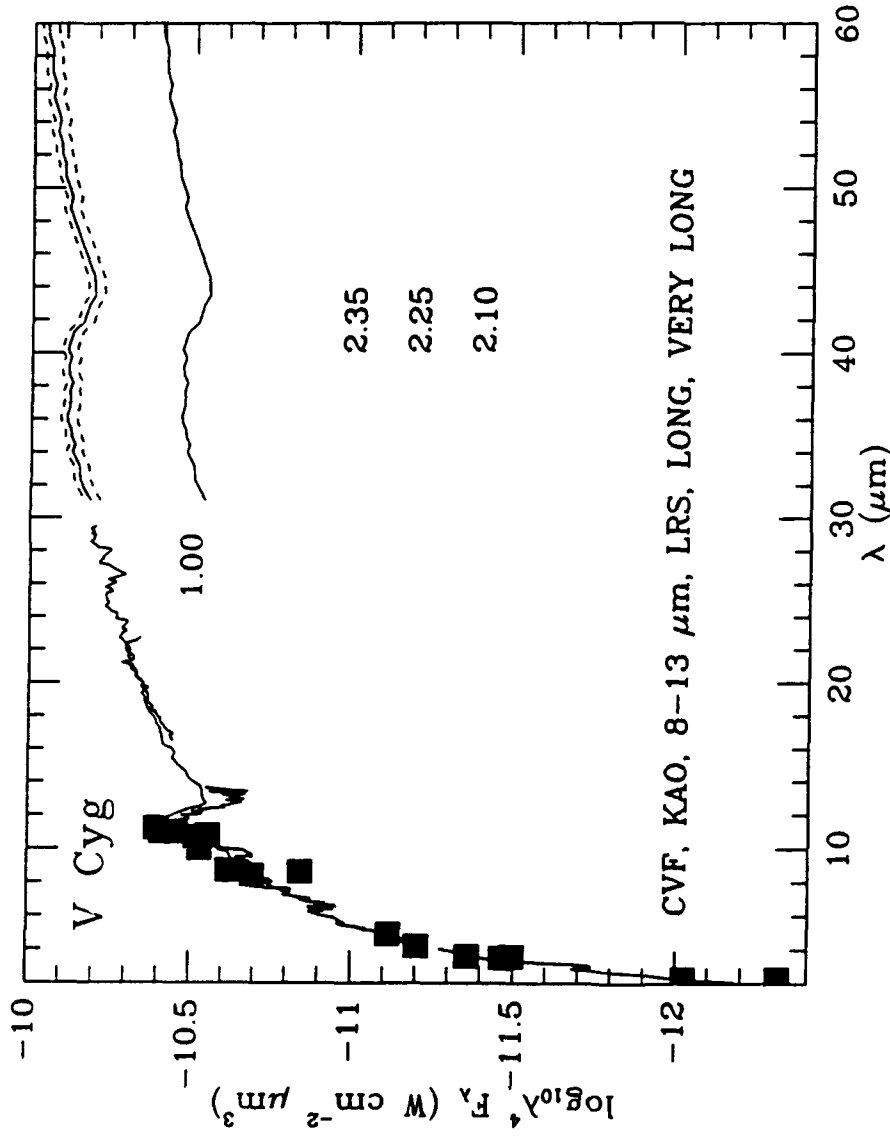


Fig. 1: f) final merging with the longest wavelength KAO data (from ~ 30 - $60 \mu\text{m}$) taken at a different epoch from the other fragments and published only in relative units. Best fit factor 2.25, with range 2.10-2.35 (dashed curves).

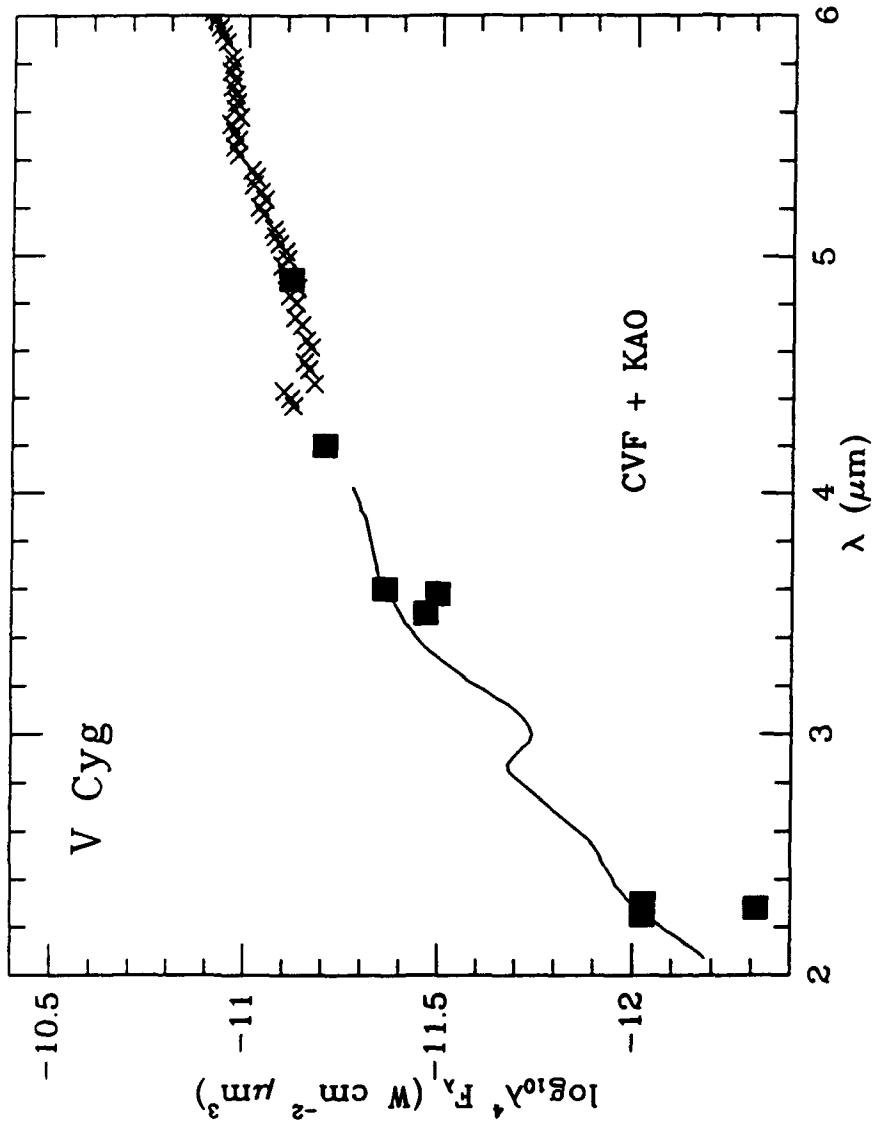


Fig. 1: g) splicing of CVF and KAO spectral fragments after each has been rescaled.

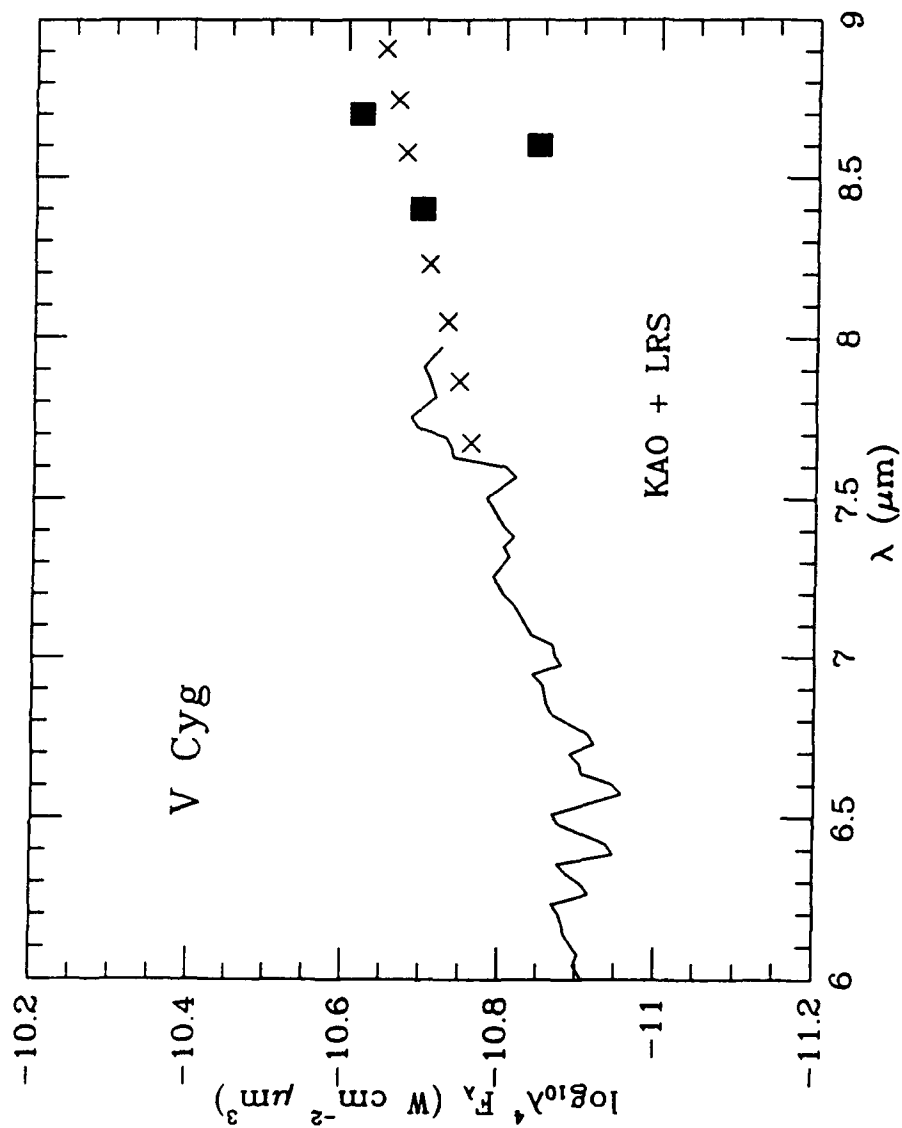


Fig. 1: h) same for KAO and LRS (the 8-13 μm spectra were used primarily as a check on the LRS level and shape: the LRS was always preferable because of its broader wavelength coverage).

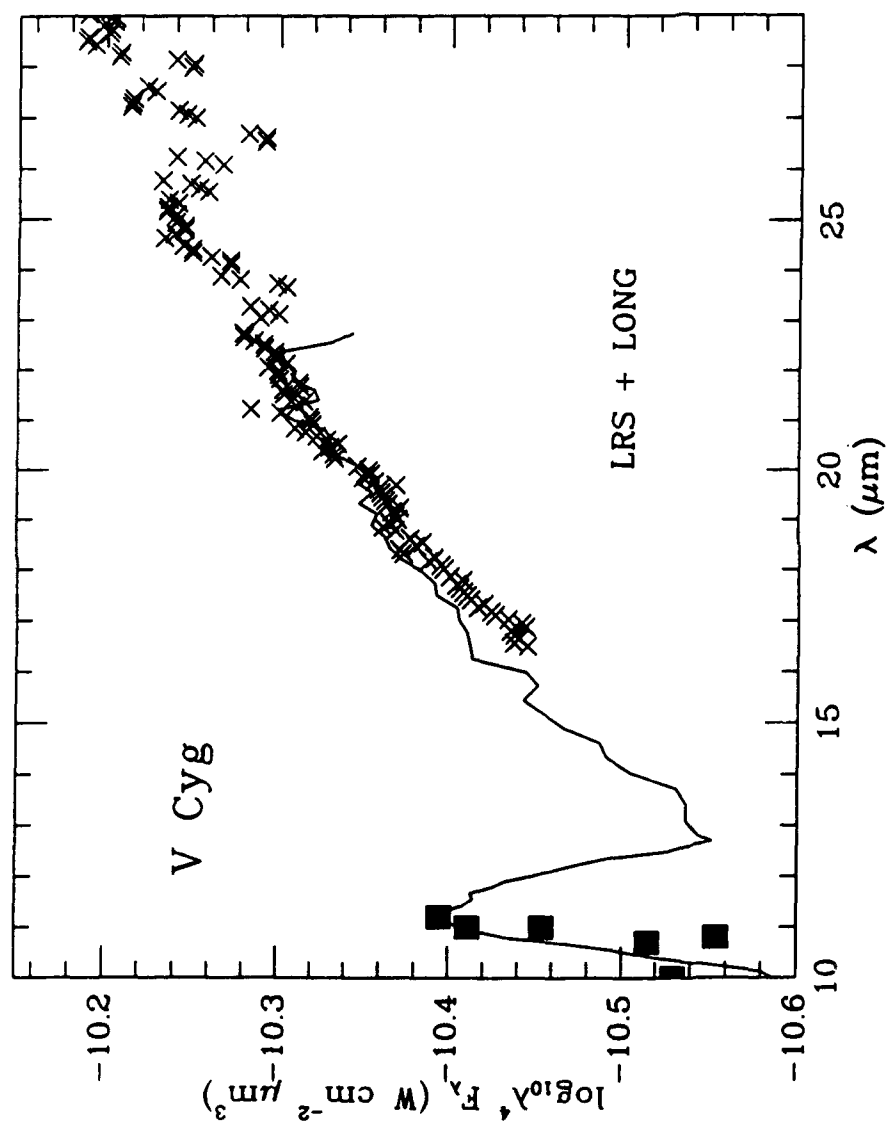


Fig. 1: i) same for LRS and long KAO fragments.

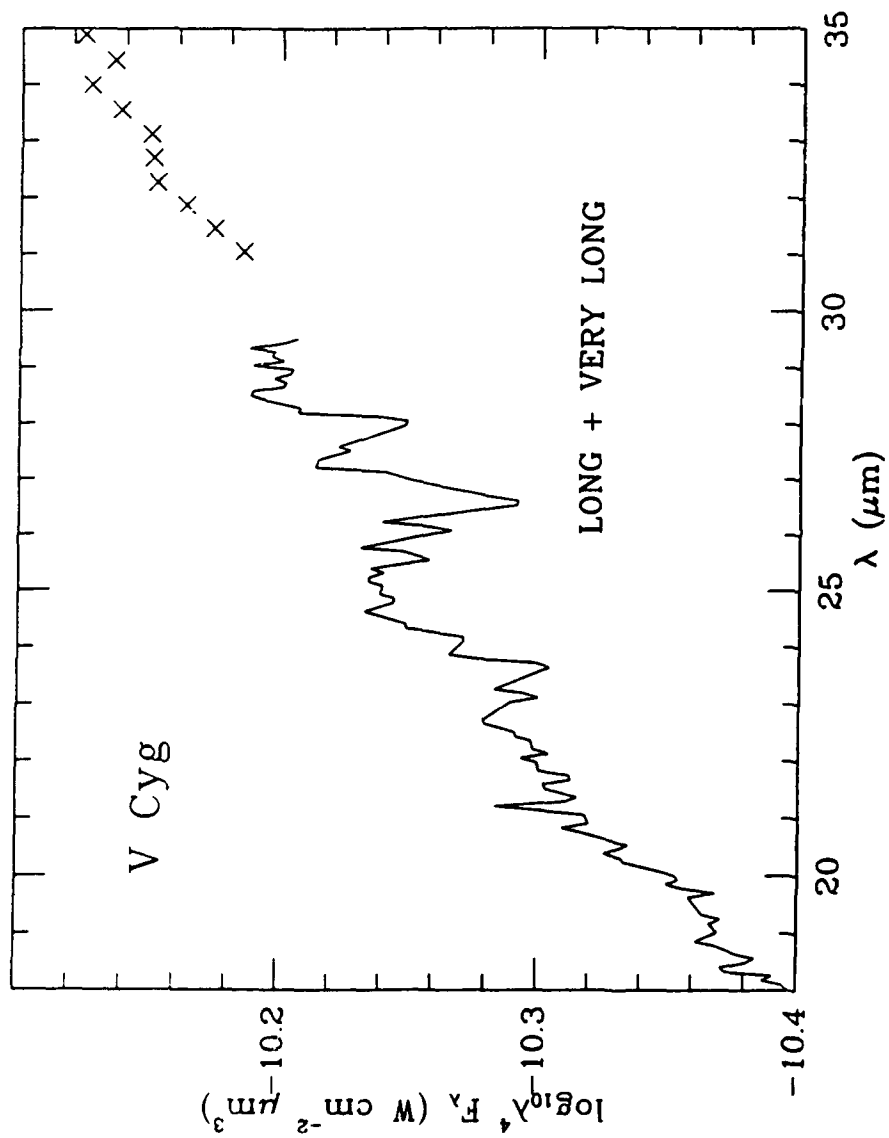


Fig. 1: j) same for long and very long KAO fragments.

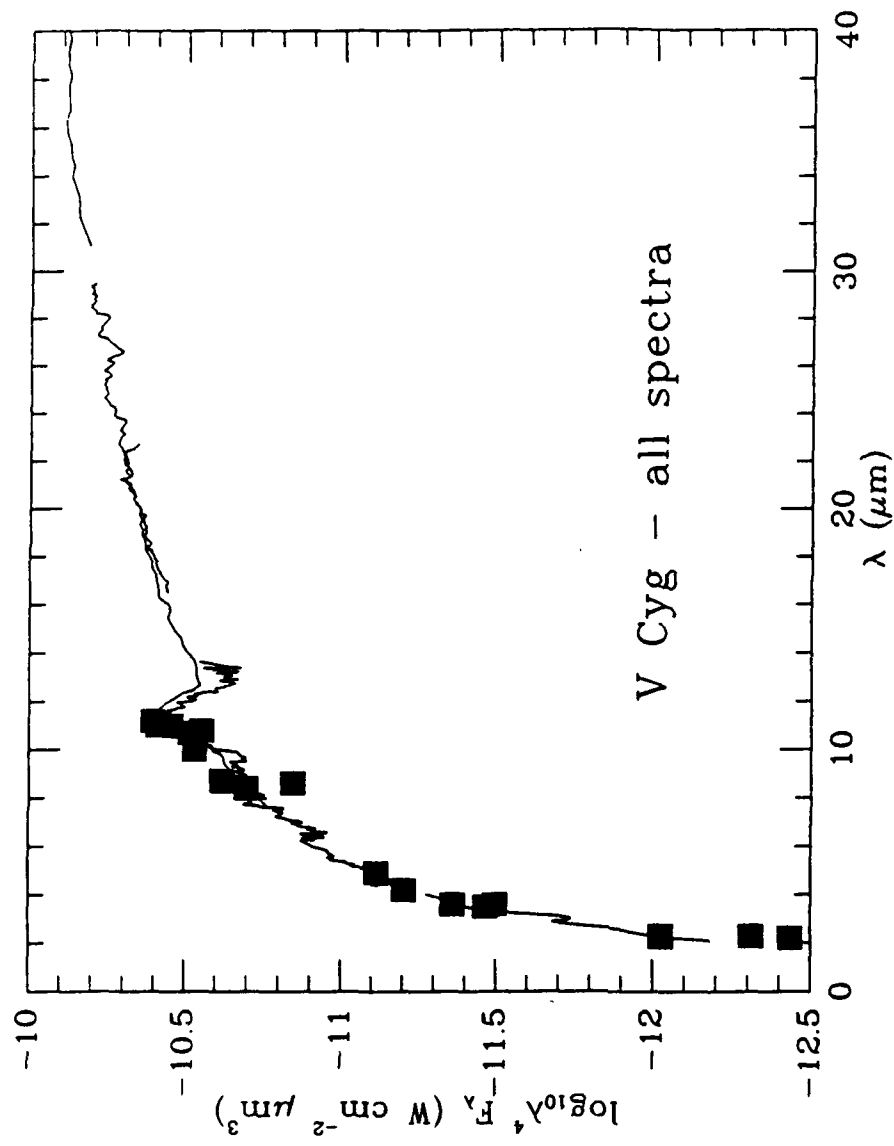


Fig. 1: k) composite of all the overlapping spectral fragments and photometry.

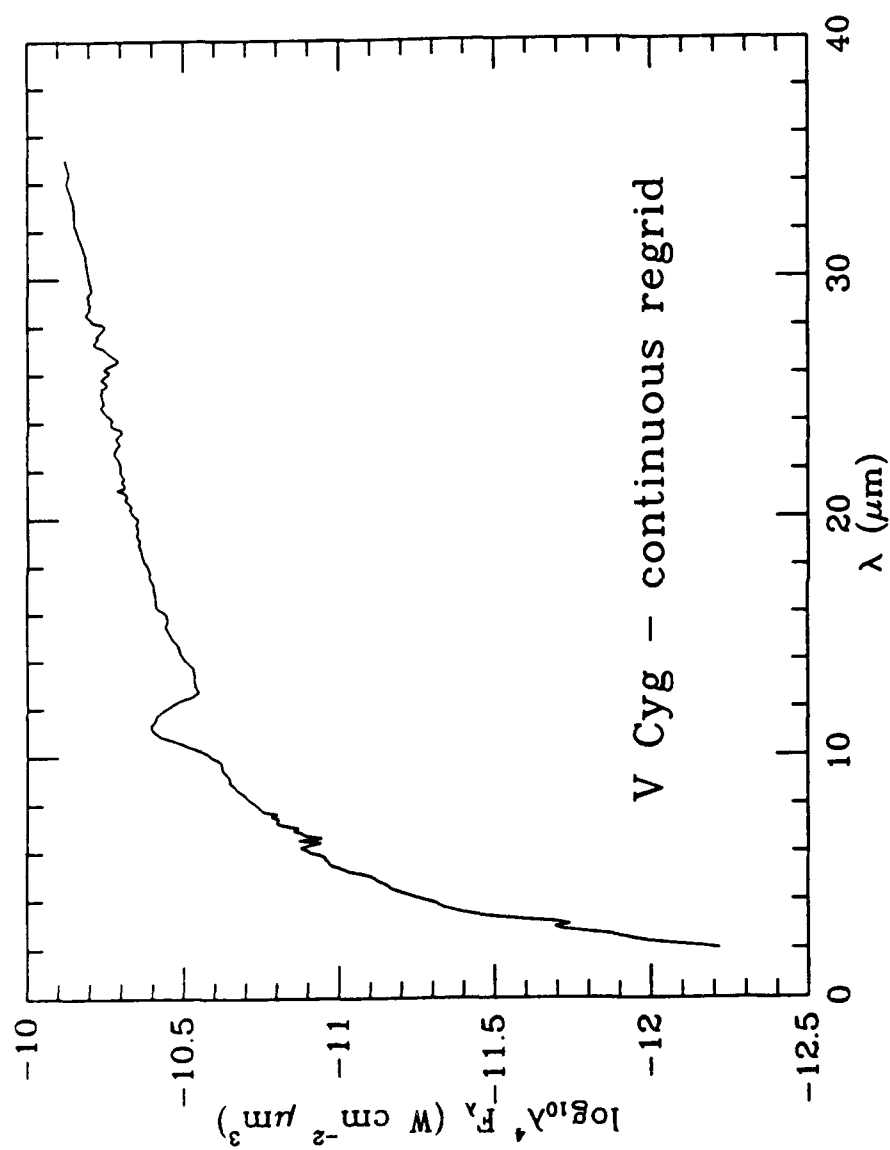


Fig. 1: 1) complete 2-35 μm spectrum with regridding of the wavelength scale by interpolation (no smoothing or cleaning has yet been performed).

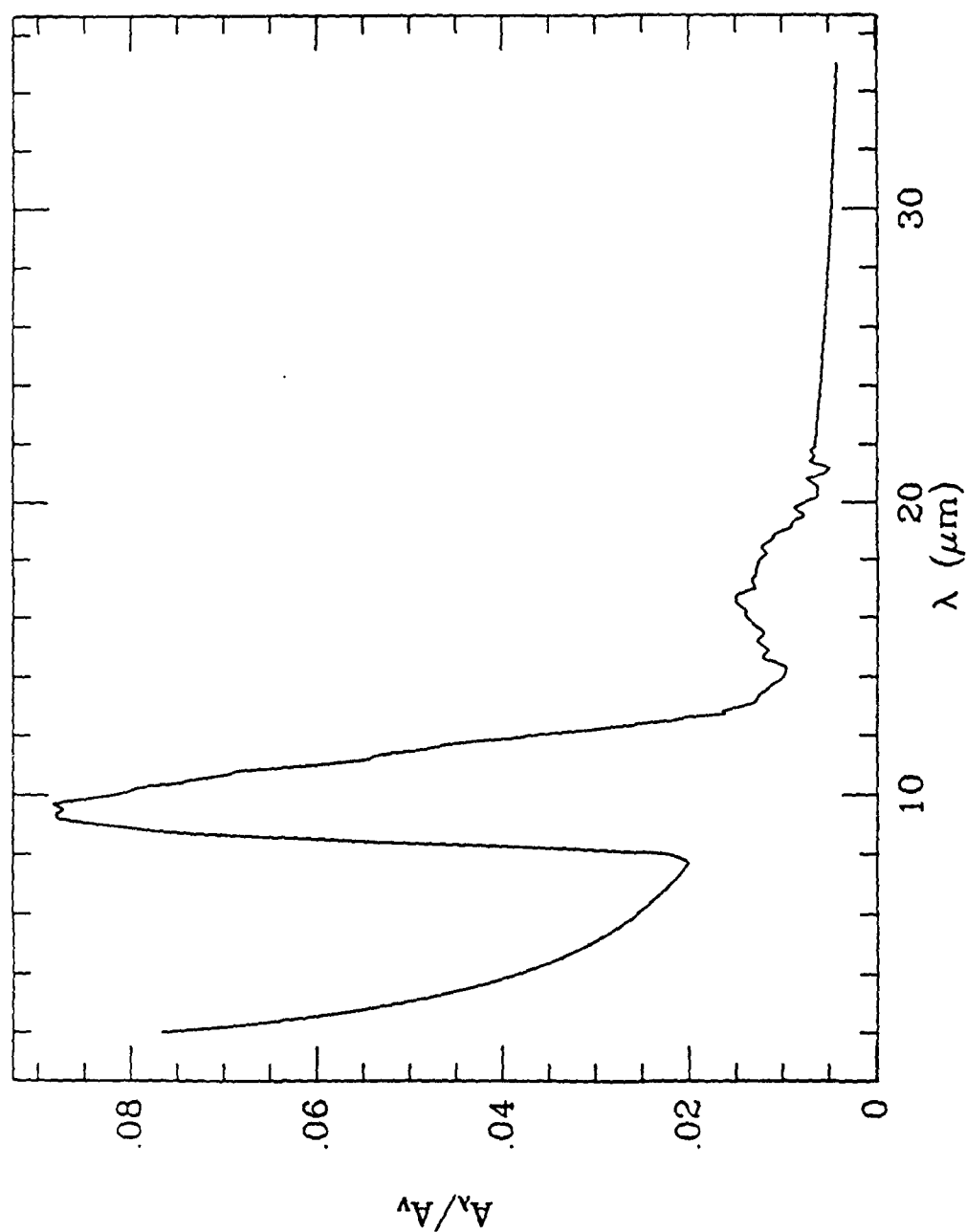


Fig. 2: The complete extinction curve from 2-35 μm with its interstellar silicate features near 10 and 20 μm , van der Hulst #15 extrapolation between 7.67 and 2.0 μm , and λ_{-1} extrapolated component (that underlies the silicate features too) beyond 22.7 μm .

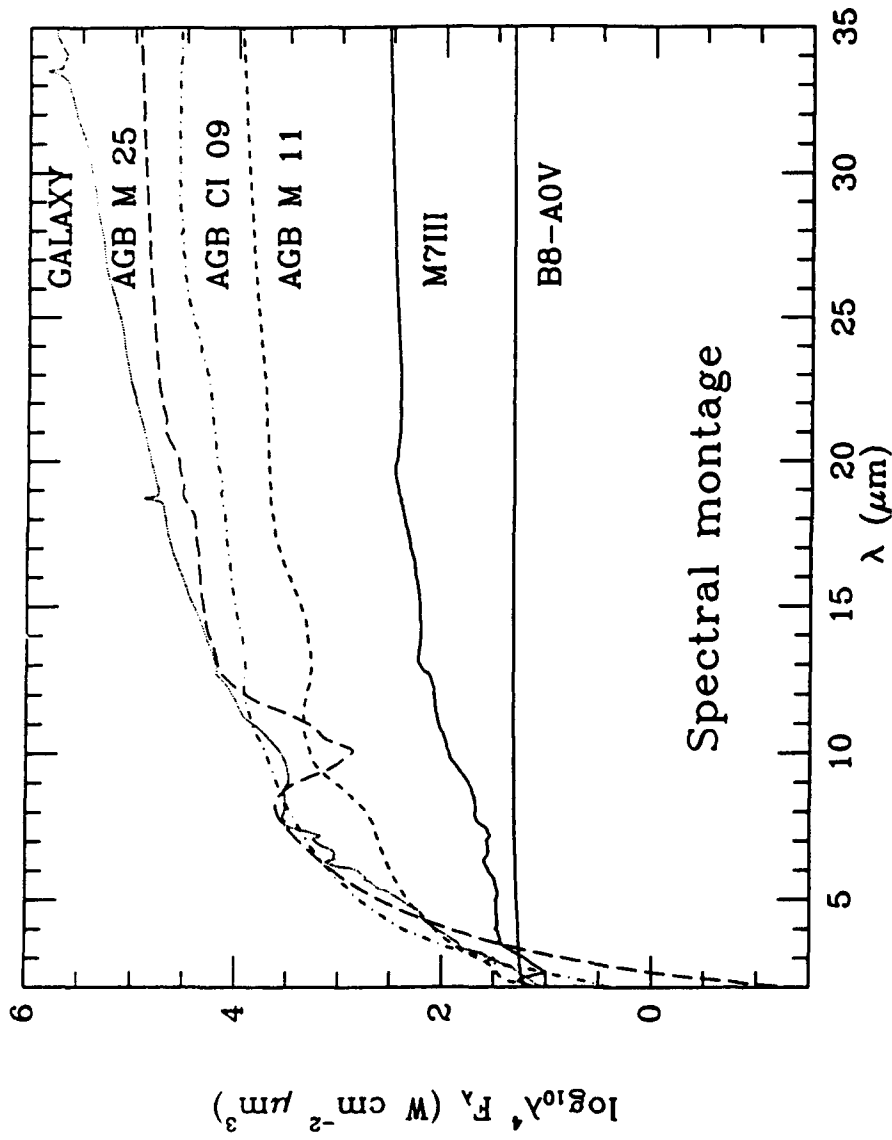


Fig. 3: Montage of several different intrinsic templates (after dereddening and smoothing have been applied).

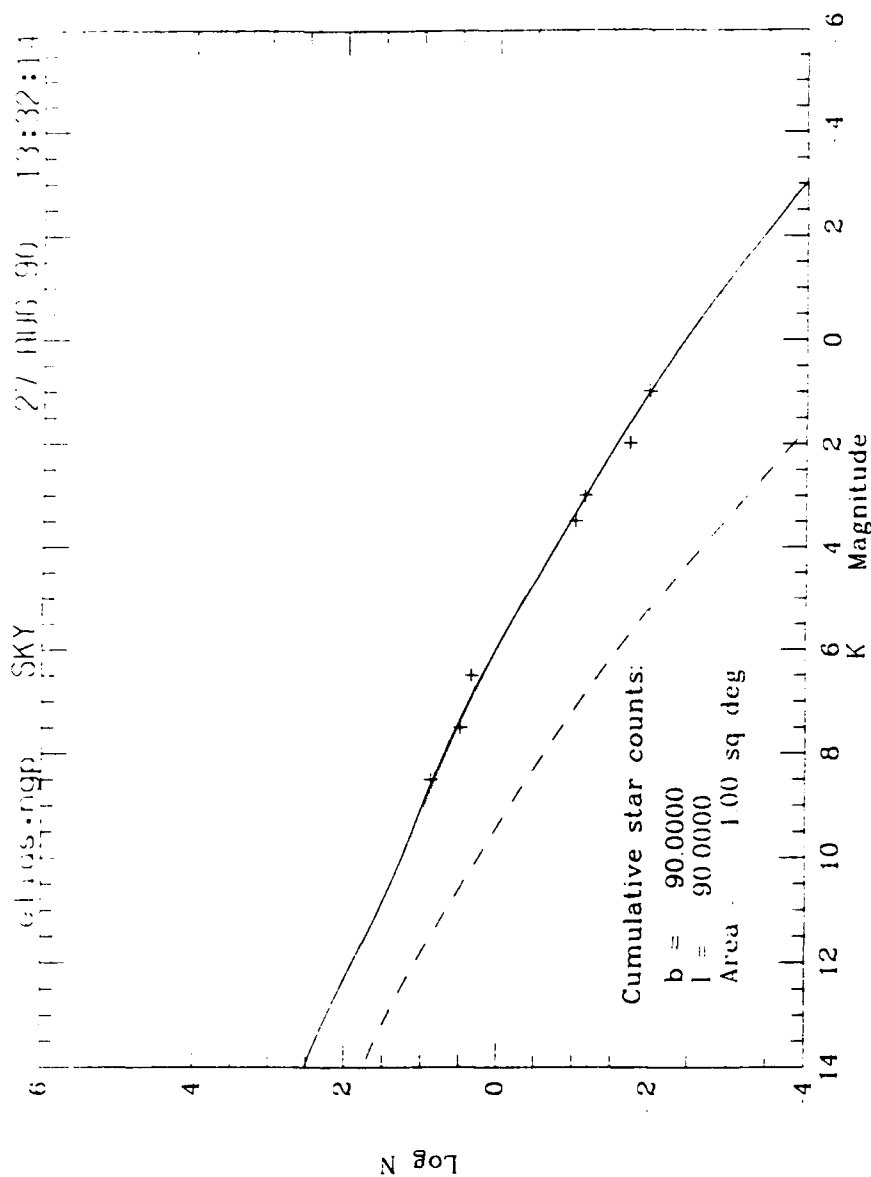


Fig. 4: Model predictions for (Log N, Log S) cumulative source counts. The different components in the model are represented as follows: total of all contributors, solid line; disk, dots; short dash, bulge; long dash, spiral arms; dot-short dash, molecular ring; dot-long dash, halo; short dash-long dash, external galaxies. Predictions for the north galactic pole compared with Elias (1978) actual counts (observational counts are represented by crosses).

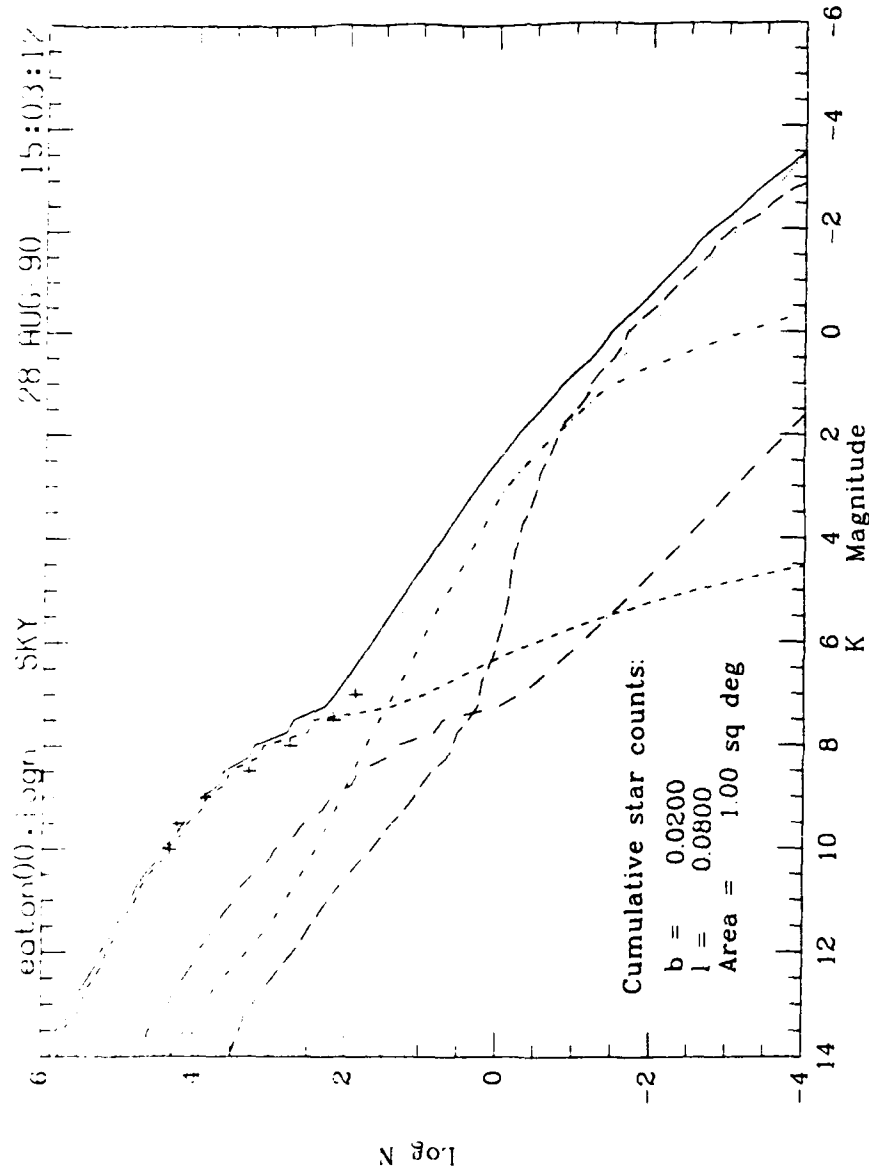


Fig. 5a: As in Fig. 4 but for one small area in the Galactic plane studied by Eaton, Adams, and Giles (1984).

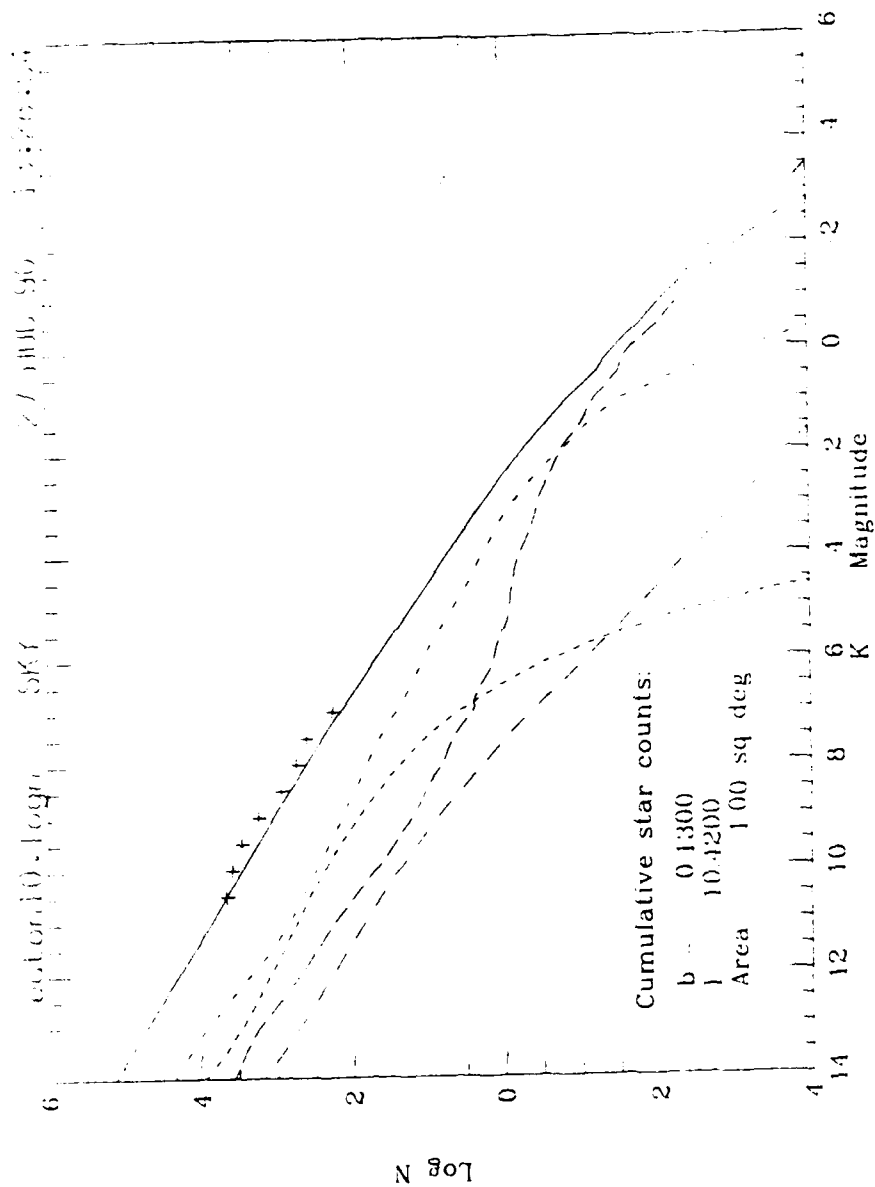


Fig. 5b: As in Fig. 4 but for one small area in the Galactic plane studied by Eaton, Adams, and Giles (1984).

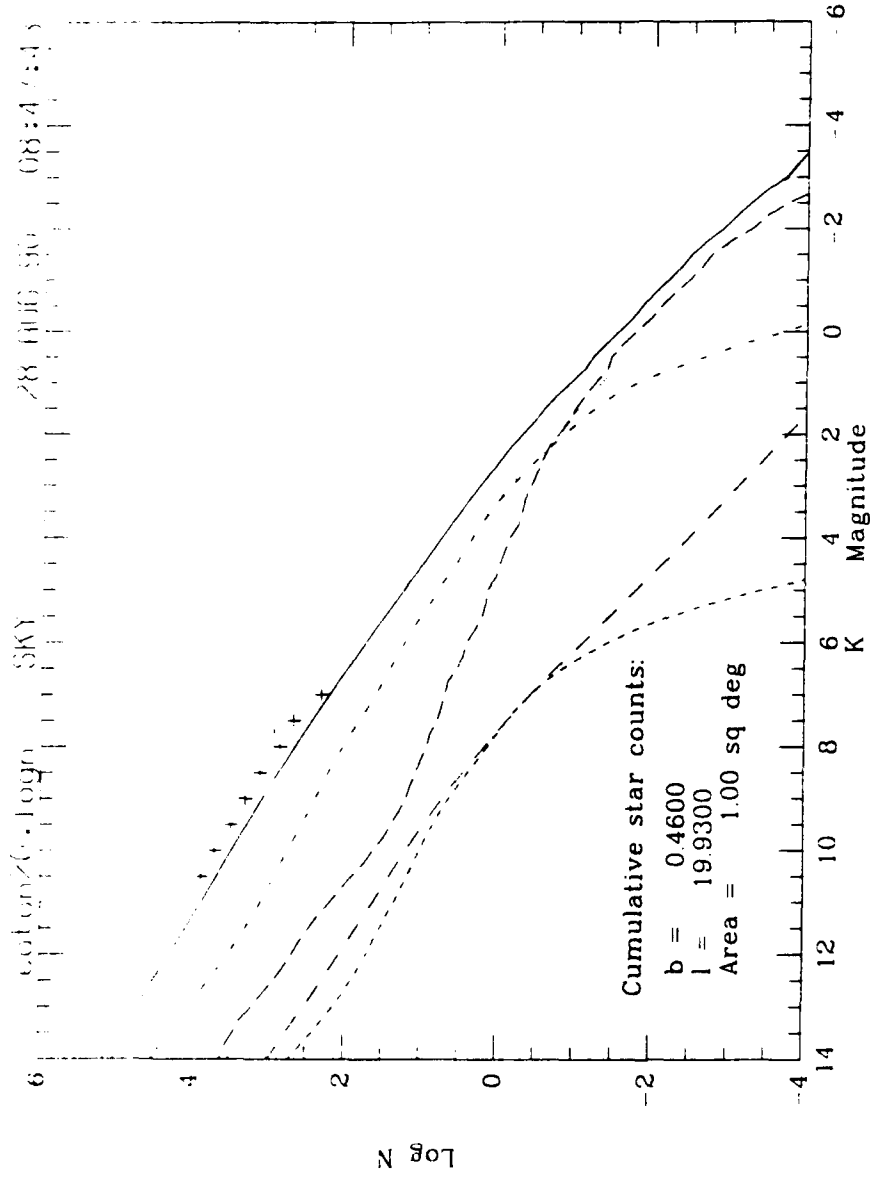


Fig. 5c: As in Fig. 4 but for one small area in the Galactic plane studied by Eaton, Adams, and Giles (1984).

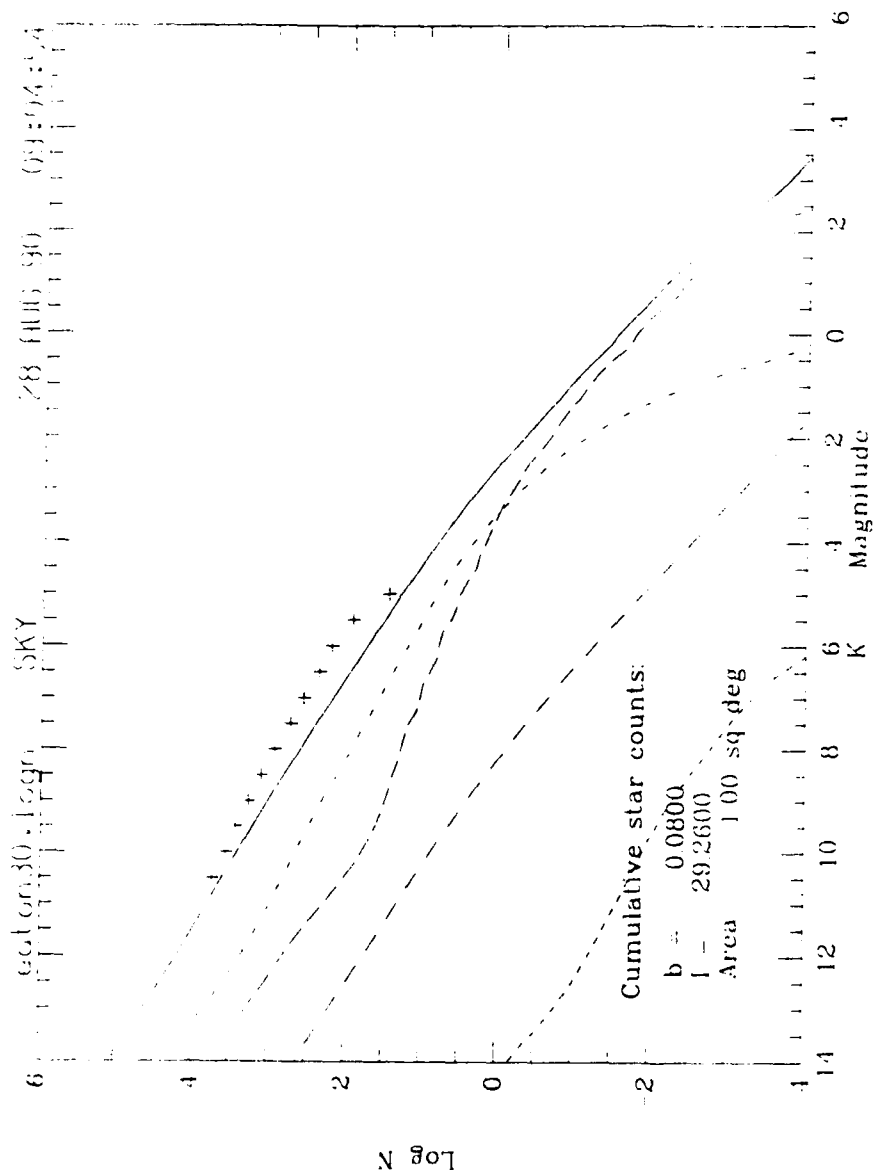


Fig. 5d: As in Fig. 4 but for one small area in the Galactic plane studied by Eaton, Adams, and Giles (1984).

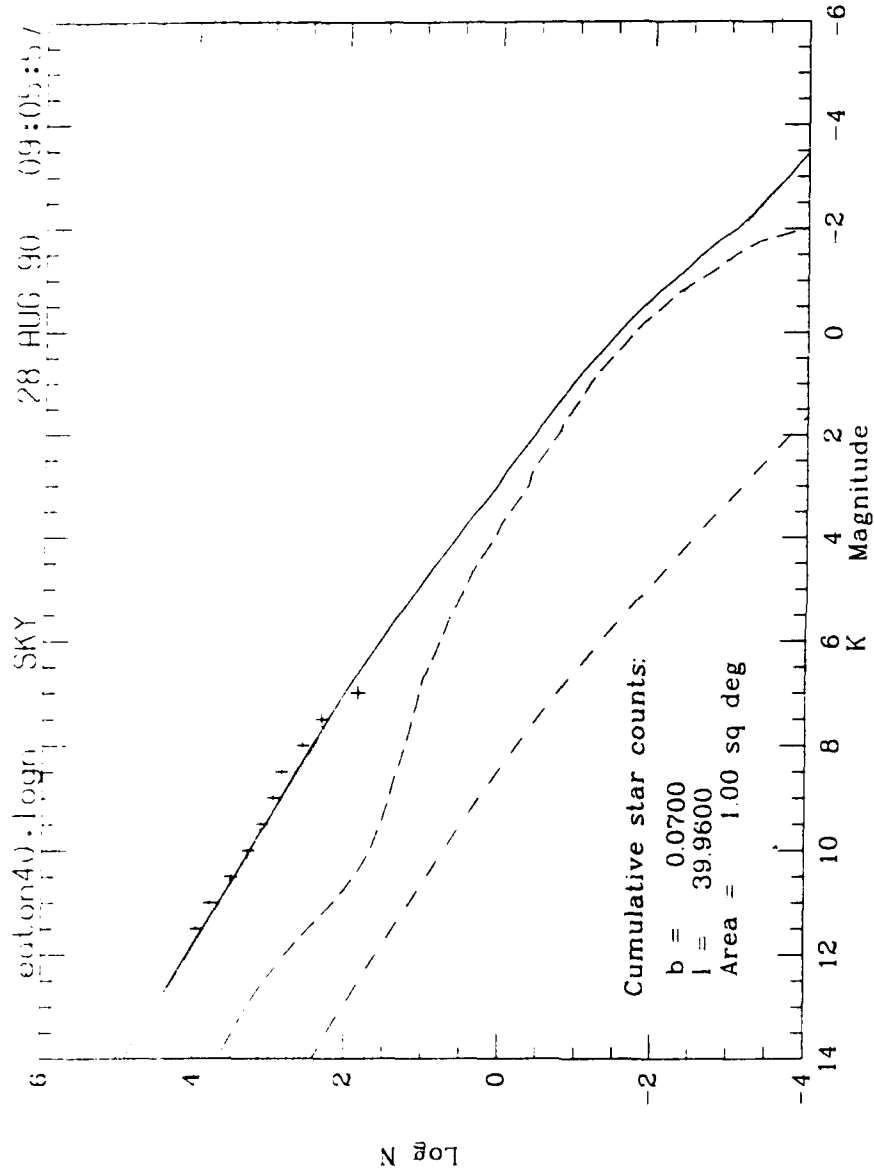


Fig. 5e: As in Fig. 4 but for one small area in the Galactic plane studied by Eaton, Adams, and Giles (1984).

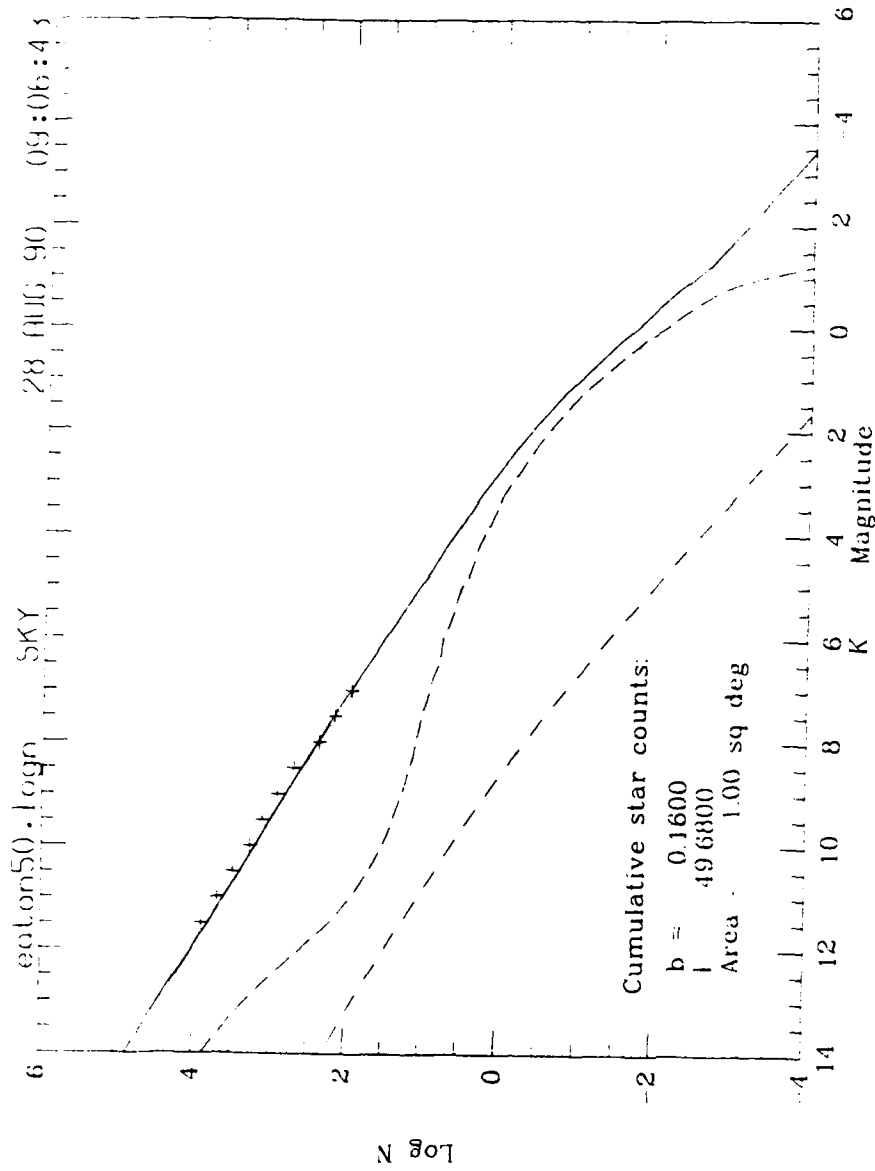


Fig. 5f: As in Fig. 4 but for one small area in the Galactic plane studied by Eaton, Adams, and Giles (1984).

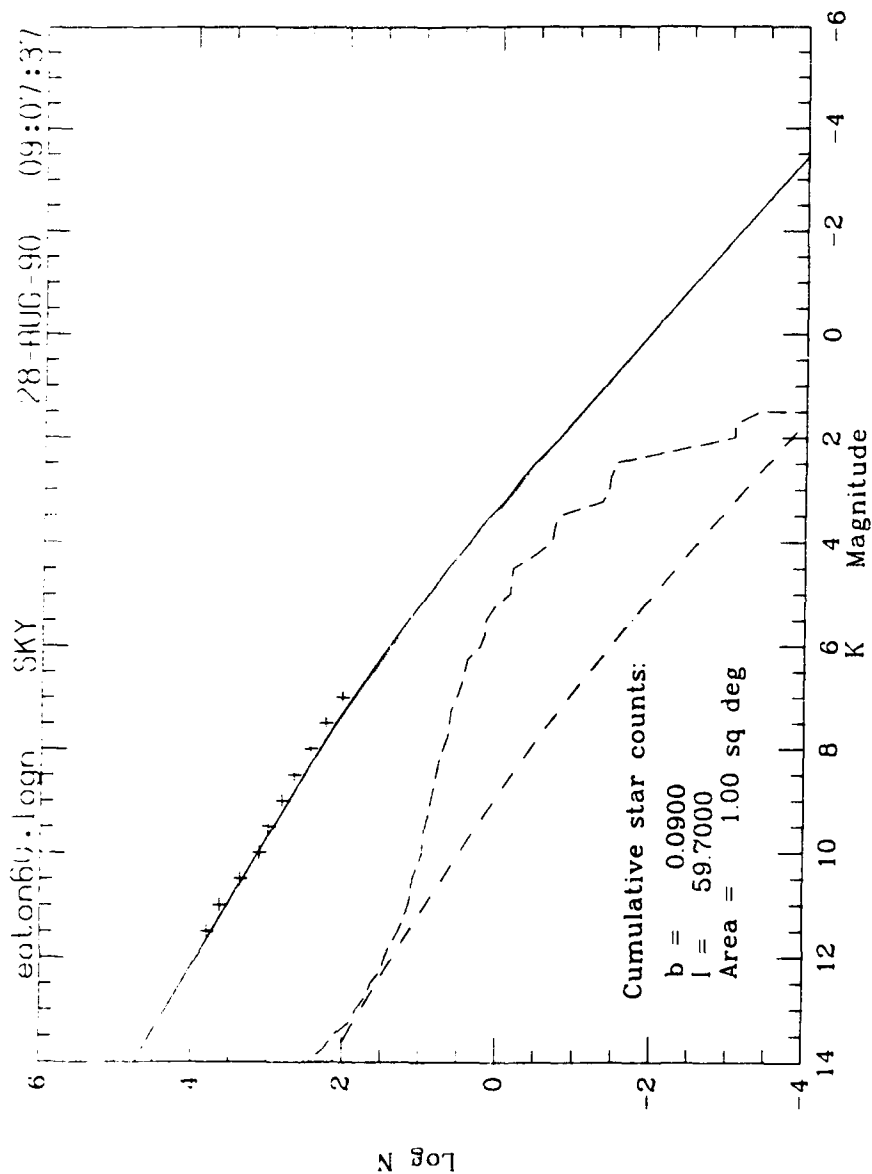


Fig. 5g: As in Fig. 4 but for one small area in the Galactic plane studied by Eaton, Adams, and Giles (1984).

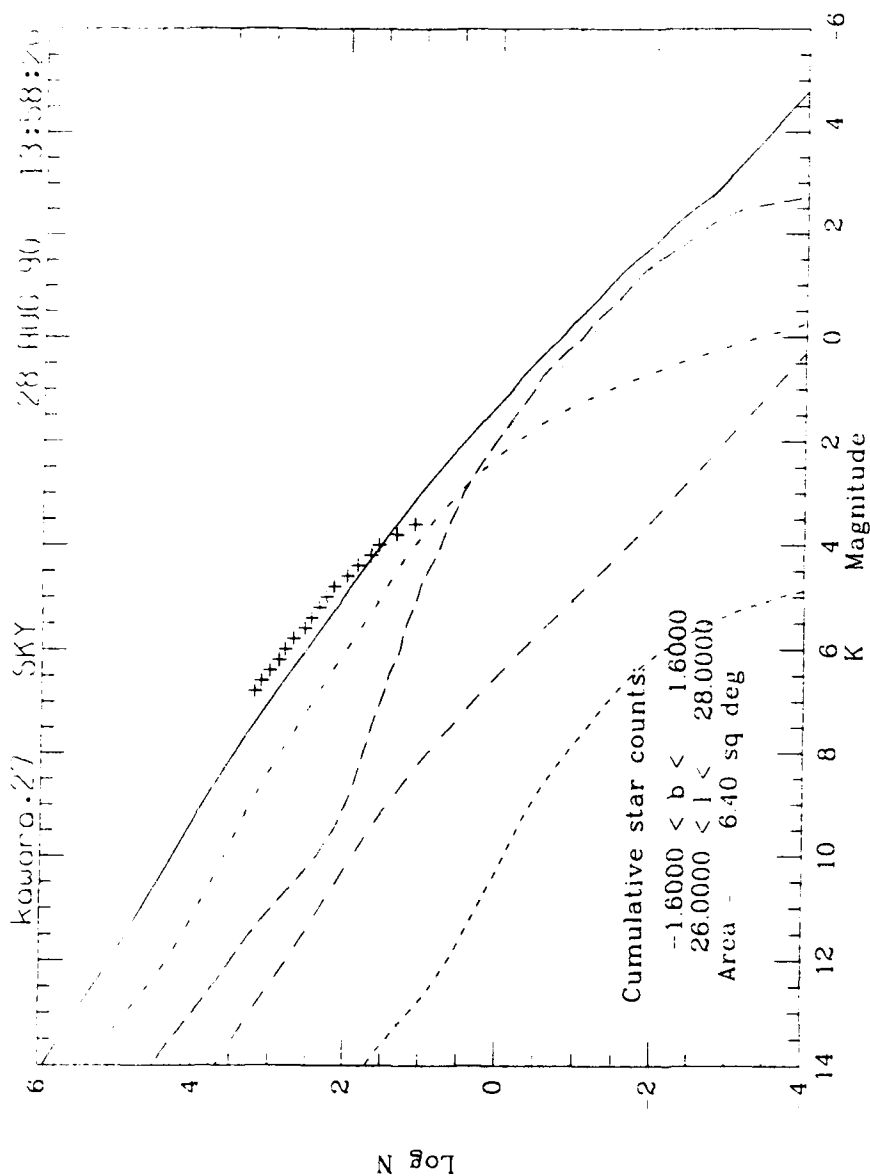


Fig. 6: As in Fig. 5 but for the Galactic plane zones observed by Kawara et al. (1982); the four zones involving contiguous areas are shown (crosses represent the observed cumulative counts).

Fig. 6a: For the zone near 27° longitude, the Model was run in its "integrate over area" mode, gridding the latitude range uniformly with step 0.8° , and longitude with step 0.5° (i.e. the sum of 16 separate calculations).

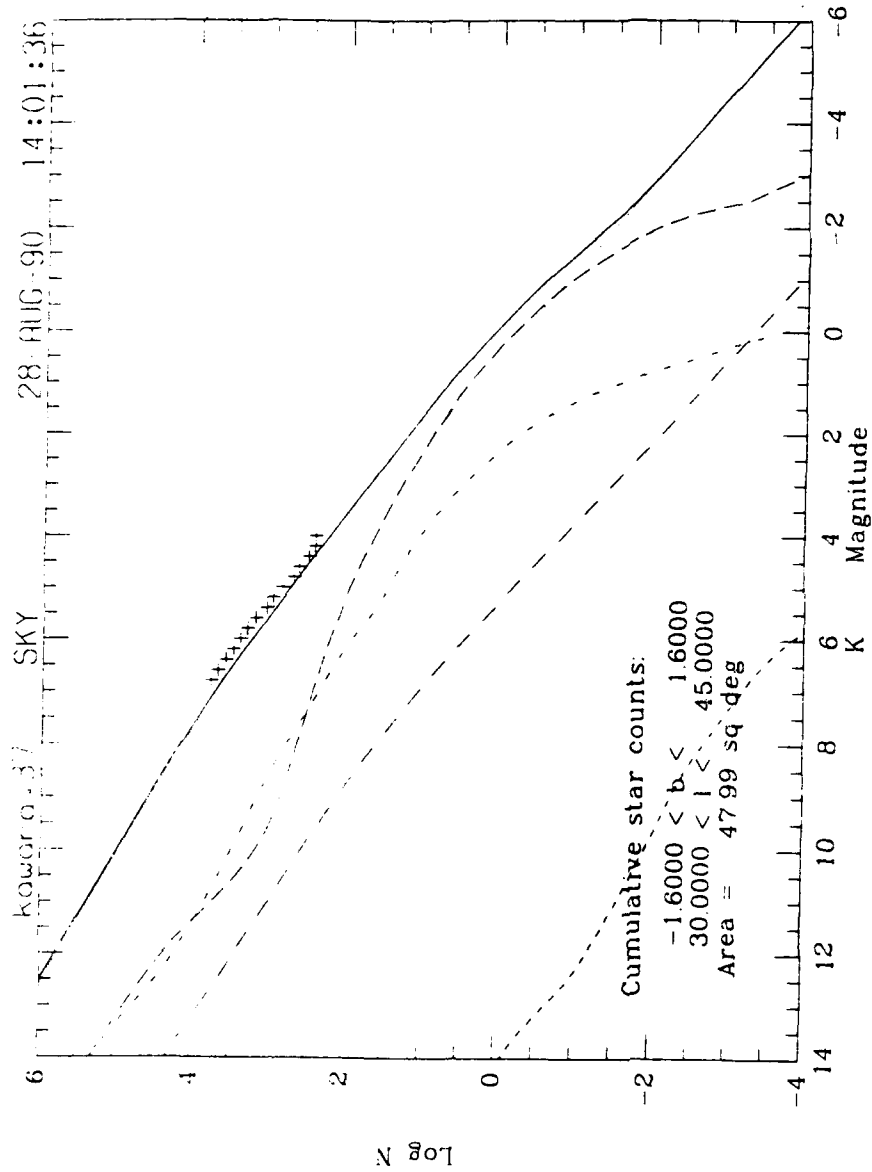


Fig. 6b: The zone centered near $l=37^\circ$ was gridded in latitude by 0.8° and longitude by 5° (i.e. the sum of 12 calculated rays).

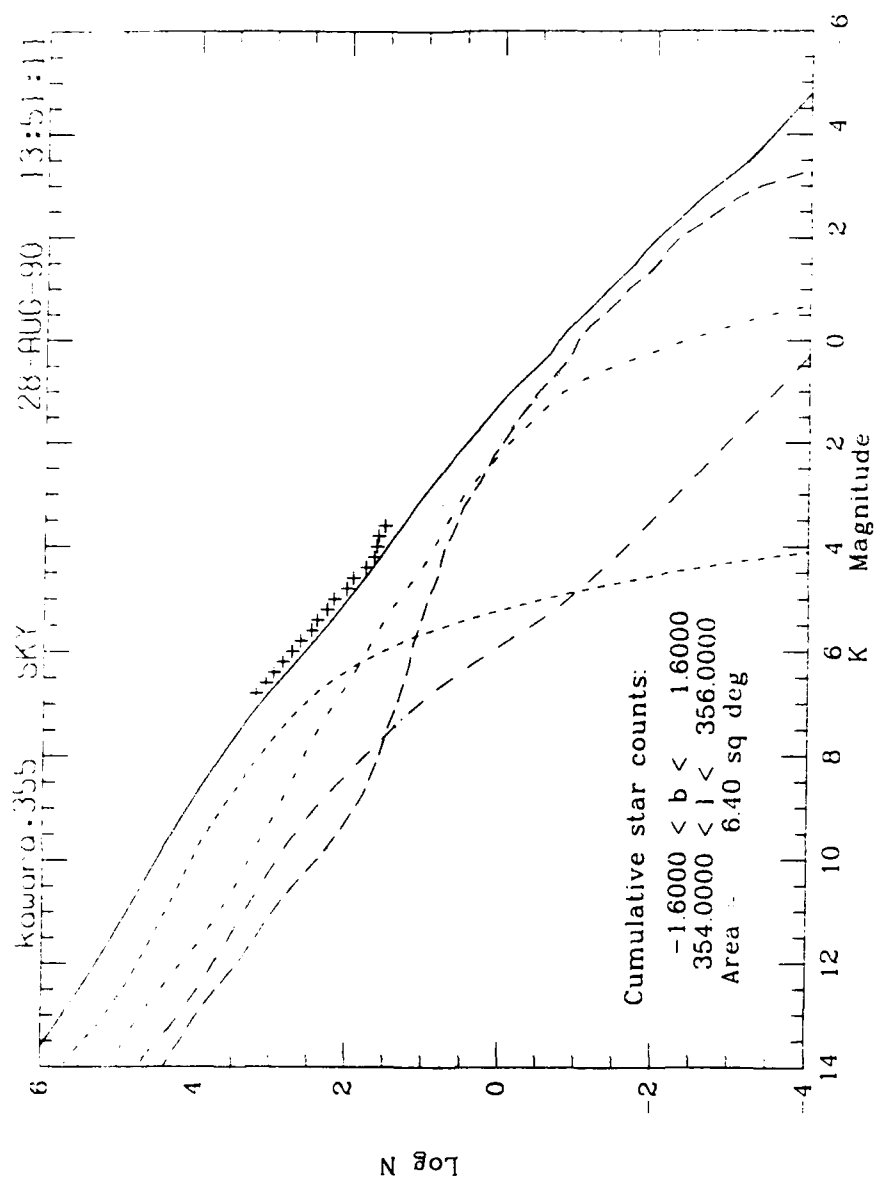


Fig. 6c: The zone centered on $l=355^\circ$ was similarly the sum of 16 calculated rays (steps in latitude and longitude of 0.8° and 0.5° , respectively).

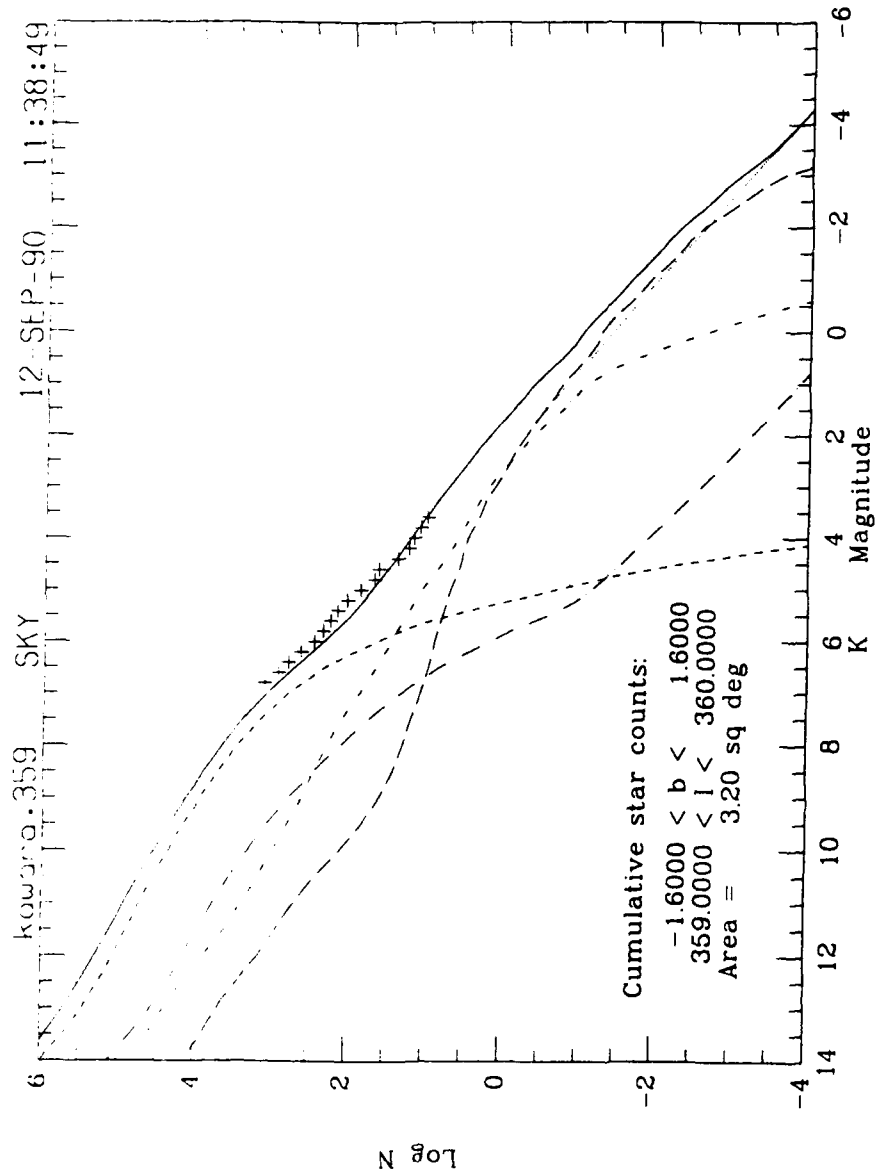


Fig. 6d: The zone centered on $l=359^\circ$ summed 16 rays with steps of 0.4° and 0.5° , respectively.

Table 1. The categories of source used in the Sky Model and the individual objects and their spectral fragments that were chosen to represent them. IRAS LRS spectra exist for all sources except those whose names are followed by an asterisk. {} denote sources whose spectra were not used in the creation of the average template for their category.

Category/ Source/LRS?	Total Range (μm)	References
<u>B0.1 V</u> { ζ Oph} α Vir	1.3-2.6, 2.6-4.0	Strecker (unpublished archive) used photometry, LRS, and blackbody
<u>B2.3 V</u> {102 Her} α Eri	1.2-2.5, 2.9-4.0	Bregman & Witteborn (unpublished) used photometry, LRS, and blackbody
<u>B5 V</u> α Leo α Gru	2.0-5.70	Bregman & Witteborn (unpublished) used photometry, LRS, and blackbody
<u>B8-A0 V</u> α CMa	1.2-4.1	Strecker et al. 1979
<u>A2-5 V</u> α Gem α Psa		used photometry, LRS, and blackbody used photometry, LRS, and blackbody
<u>F0-5 V</u> α Aql α CMi		used photometry, LRS, and blackbody used photometry, LRS, and blackbody
<u>F8 V</u> { θ Per} β Vir 44 Dra β Cap	1.2-2.5, 2.9-4.0	Bregman & Witteborn (unpublished) used photometry, LRS, and blackbody used photometry, LRS, and blackbody used photometry, LRS, and blackbody
<u>G0-2 V</u> BS 2721 α Cen		used photometry, LRS, and blackbody used photometry, LRS, and blackbody
<u>G5 V</u> δ Pav		used photometry, LRS, and blackbody
<u>G8-K3 V</u> BS 8832 HR 365 Gliese 324A	1.2-2.5, 2.9-4.0	Bregman & Witteborn (unpublished) used photometry, LRS, and blackbody used photometry, LRS, and blackbody
<u>K4-5 V</u> 61 Cyg A Gliese 365		used photometry, LRS, and blackbody used photometry, LRS, and blackbody
<u>M0-1 V</u>		

[Gliese 15A] Gliese 546 HD 36395	1.2-2.5, 2.9-4.0	Bregman & Witteborn (unpublished) used photometry, LRS, and blackbody used photometry, LRS, and blackbody
<u>M2-3 V</u>		
Gliese 411	1.3-2.5, 2.9-4, 8-13	Berriman and Reid 1987
<u>M4-5 V</u>		
[Gliese 447*] Gliese 699* Gliese 752A*	2.9-4.0 1.3-2.5, 2.9-4.0 1.3-2.5, 2.9-4.0	Berriman and Reid 1987 Berriman and Reid 1987 Berriman and Reid 1987
<u>M-late V</u>		
Gliese 406* Gliese 866* GJ 1111*	1.3-2.5, 2.9-4, 8-13 1.3-2.5, 2.9-4.0 1.3-2.5, 2.9-4.0	Berriman and Reid 1987 Berriman and Reid 1987 Berriman and Reid 1987
<u>F8-G2 III</u>		
α Aur ϵ Leo	1.2-2.3, 3.0-4.1 4.5-5.6	Bregman (unpublished) used photometry, LRS, and blackbody
<u>G5 III</u>		
α Aur σ UMa	1.2-2.3, 3.0-4.1 4.5-5.6	Bregman (unpublished) used photometry, LRS, and blackbody?
<u>G8 III</u>		
η Dra κ Cyg		used photometry, LRS, and blackbody Bregman & Witteborn (unpublished)
<u>K0,1 III</u>		
β Gem α UMa α Boo	1.2-4.2, 4.5-5.7 1.2-4.1, 4.5-5.2 1.2-4.3	Strecker et al. 1979 Strecker et al. 1979 Strecker et al. 1979
<u>K2,3 III</u>		
γ And	1.2-2.4, 2.9-4.2, 4.5-5.5	Strecker et al. 1979
<u>K4,5 III</u>		
α Tau	1.2-4.2, 4.5-5.5 3.0-5.6 20.0-35.1	Strecker et al. 1979 Bregman (unpublished) Glaccum 1990
<u>M0 III</u>		
μ Uma δ And	2.1-2.5, 2.8-4.0 1.2-4.2, 4.5-5.5	Merrill and Stein 1976a Strecker et al. 1979
<u>M1 III</u>		
α Cet	1.3-2.4, 2.9-4.2, 4.5-5.7	Strecker et al. 1979
<u>M2 III</u>		
δ Peg	1.2-4.2, 4.5-5.7	Strecker et al. 1979

<u>M3 III</u>		
δ Vir	2.1-2.5, 2.9-4.0	Merrill and Stein 1976a
<u>M4 III</u>		
δ^2 Lyr	2.9-4.0	Noguchi et al. 1977
ρ Per	2.9-4.0	Noguchi et al. 1977
<u>M5 III</u>		
TU CVn	1.2-2.4, 2.9-5.4 2.0-2.5	Strecker (unpublished) Arnaud et al. 1989
<u>M6 III</u>		
RZ Ari	2.1-2.5, 2.9-4.0	Merrill and Stein 1976a
g Her	1.2-2.6, 2.6-4.0 8-13	Strecker (unpublished) Merrill and Stein 1976a
<u>M7 III</u>		
RX Boo	2.1-2.5, 2.9-4.0 5.1-7.8 15.7-30.1 20.0-35.1	Merrill and Stein 1976a Bregman (unpublished) Forrest, McCarthy, and Houck 1979 Glaccum 1990
<u>YOUNG OB</u>		
γ^2 Vel	1.4-2.5, 2.8-4.2, 7.9-13.3	Aitken, Roche, and Allen 1982
β Ori	1.2-2.5, 2.9-4.0	Bregman and Witteborn (unpublished)
P Cyg	1.2-2.6, 2.6-4.3	Strecker (unpublished)
<u>A-G I-II</u>		
α Cyg	2.0-5.70	Bregman and Witteborn (unpublished)
α UMi	1.2-4.2, 4.5-5.6	Strecker et al. 1979
β Dra	1.2-4.3	Strecker et al. 1979
<u>K-M2 I-II</u>		
α Ori	2.1-2.5, 2.9-4.0, 4.5-13.6 15.9-38.4 20.0-35.1	Puetter et al. 1977 Forrest, McCarthy, and Houck 1979 Glaccum 1990
μ Cep	2.1-2.5, 2.8-4.0, 4.5-13 15.7-30.1 20.0-35.1	Merrill and Stein 1976a Forrest, McCarthy, and Houck 1979 Glaccum 1990
α Sco	1.2-2.6, 2.6-4.0 4-8 20.0-35.1	Strecker (unpublished) Bregman and Witteborn (unpublished) Glaccum 1990
<u>M3-4 I-II</u>		
α^1 Her	1.2-2.6, 2.6-4.0 5.3-8.0 19.9-35.0	Strecker (unpublished) Cohen (unpublished) Glaccum 1990
[RW Cyg]	2.1-2.5, 2.8-4.0, 8.0-13.0	Merrill and Stein 1976a

R Lyr	2.9-4.1	Noguchi et al. 1977
TU CVn	2.0-2.5	Arnaud et al. 1989
<u>AGB M 03</u>		
R Leo	1.2-4.1	Strecker, Erickson, and Witteborn 1978
	8.0-13.0	Merrill and Stein 1976a
	20.0-35.1	Glaccum 1990
<u>AGB M 05</u>		
R Cas	1.2-4.1	Strecker, Erickson, and Witteborn 1978
	2.1-2.5, 2.9-4.0,	
	4.5-13.6	Puetter et al. 1977
	15.7-30.1	Forrest, McCarthy, and Houck 1979
	20-35	Glaccum 1990
TX Cam	2.1-2.5, 2.9-4.0,	
	8.0-13.0	Merrill and Stein 1976b
	3.0-5.6	Bregman (unpublished)
R LMi	5.3-8.0	Cohen (unpublished)
<u>AGB M 07</u>		
RS Cnc	2.1-2.5, 2.8-4.0,	
	8.0-13	Merrill and Stein 1976a
o Cet	2.1-2.5, 2.9-4.0,	
	8.0-13.0	Merrill and Stein 1976a
	4.4-5.4	Scargle and Strecker 1979
	16.3-29.1	Glaccum 1990
<u>AGB M 09</u>		
NML Tau	1.2-4.1	Strecker, Erickson, and Witteborn 1978
	20.0-35.1	Glaccum 1990
GL 1141	2.1-2.5, 2.9-4.0,	
	8-12.5	Merrill and Stein 1976b
X Her	15.7-30.0	Forrest, McCarthy, and Houck 1979
	20.1-35.2	Glaccum 1990
+70066	1.2-2.4, 2.9-5.6	Strecker (unpublished)
<u>AGB M 11</u>		
+40149	2.1-2.5, 2.9-4.0,	
	8-12.6	Merrill and Stein 1976b
GL 2241	2.0-2.5, 2.8-4.0,	
	7.8-13.3	Cohen (unpublished)
	6.4-7.7	Bregman and Witteborn (unpublished)
CIT 1	2.1-2.5, 2.9-4.0,	
	8-12.8	Merrill and Stein 1976b
WX Ser	1.4-2.5, 2.9-3.8	Jones et al. 1988
<u>AGB M 13</u>		
+00102	2.1-2.5, 2.9-4.0,	
	8-12.5	Merrill and Stein 1976b
+10011	2.1-2.5, 2.9-4.0,	
	8-13.2	Merrill and Stein 1976b
+20326	2.1-2.5, 2.9-4.0,	
	8-13.3	Merrill and Stein 1976b
GL 1686	2.4-8.0	Bregman and Witteborn (unpublished)
	8.0-13.0	Merrill and Stein 1976c

<u>AGB M 15</u>		
+40156	2.1-2.5, 2.9-4.0, 8.0-13.1	Merrill and Stein 1976b
<u>AGB M 17</u>		
GL 3022	2.0-2.4, 3.0-4.0, 8.0-13.1	Eiroa et al. 1981
PZ Cas	15.9-38.4	Forrest, McCarthy, and Houck 1979
<u>AGB M 19</u>		
+50137	2.1-2.5, 2.9-4.0, 8.0-13.4	Merrill and Stein 1976b
<u>AGB M 21</u>		
OH 23.1-0.3	used average of AGB M 19 and AGB M 23	used photometry, LRS, and 2 blackbodies
OH 26.2-0.6	1.4-1.8, 2.0-2.5	Jones et al. 1988
<u>AGB M 23</u>		
GL 2885	2.1-2.5, 2.9-4.0, 8.0-13.0	Merrill and Stein 1976c
	2.4-3.3	Knacke et al. 1985
OH26.5+0.6	2.1-2.5, 2.9-4.0, 4.5-37.5	Forrest et al. 1978
	2.5-3.3	Knacke et al. 1985
<u>AGB M 25</u>		
OH 35.6-0.3		used photometry, LRS, and 2 blackbodies
OH 42.3-0.2		used photometry, LRS, and 2 blackbodies
<u>AGB C 01</u>		
Y CVn	1.2-2.4, 2.9-4.1, 4.3-5.6	Goebel et al. 1978
	16.5-29.5	Forrest, Houck, and McCarthy 1981
TX Psc	1.2-2.4, 2.9-4.1	Goebel et al. 1978
<u>AGB C 03</u>		
UU Aur	1.2-2.4, 2.9-5.5	Strecker (unpublished)
	4.5-7.8	Bregman (unpublished)
V CrB	1.3-2.6, 2.6-4.2	Strecker (unpublished)
	4.4-7.8	Bregman (unpublished)
R Lep	1.2-2.6, 2.6-3.2, 2.9-5.6	Strecker (unpublished)
<u>AGB C 05</u>		
V Cyg	2.1-2.5, 2.9-4.0, 4.5-13.6	Puetter et al. 1977
	16.5-29.5	Forrest, Houck, and McCarthy 1981
	31-110	Goebel and Moseley 1985
S Cep	1.3-2.4, 2.9-4.1, 4.3-5.4	Goebel et al. 1978
	16.5-29.5	Forrest, Houck, and McCarthy 1981
	31-51	Goebel and Moseley 1985
<u>AGB C 07</u>		

V Hya	2.9-4.1	Noguchi et al. 1977
<u>AGB C 09</u>		
T Ara		used photometry, LRS, and 2 blackbodies
V644 Sco		used photometry, LRS, and 2 blackbodies
SZ Sgr		used photometry, LRS, and 2 blackbodies
<u>AGB C 11</u>		
TT Cen		used photometry, LRS, and 2 blackbodies
<u>AGB C 13</u>		used photometry, LRS, and blackbody
<u>AGB C 15</u>		used photometry, LRS, and blackbody
<u>AGB C 17</u>		used photometry, LRS, and blackbody
<u>AGB C 19</u>		
HD 100764		used photometry, LRS, and 2 blackbodies
<u>AGB C 21</u>	taken equal to AGB C 19 template	
<u>AGB C 23</u>	taken equal to AGB C 19 template	
<u>AGB C 25</u>	taken equal to AGB C 19 template	
<u>AGB CI 01</u>		
GL 527	2.1-2.5, 2.9-4.0, 8-12.9	Merrill and Stein 1976b
<u>AGB CI 03</u>		
GL 799	2.0-2.5, 2.8-4.0, 7.8-13.3	Cohen 1984
GL 933	2.1-2.5, 2.9-4.1	Merrill and Stein 1976b
<u>AGB CI 05</u>		
CIT 6/GL 1403	1.2-2.4, 2.9-5.4 2.1-2.5, 2.9-4.0, 7.8-13.4 5.6-7.6 16.5-29.5 16-30, 31-51	Strecker (unpublished) Cohen 1984 Witteborn and Bregman (unpublished) Forrest, Houck, and McCarthy 1981 Goebel and Moseley 1985
CIT 5	2.1-2.5, 2.9-4.0, 8-13.1 15.8-30 31-51	Merrill and Stein 1976b Forrest, Houck, and McCarthy 1981 Goebel and Moseley 1985
<u>AGB CI 07</u>		
GL 2232	2.1-2.5, 2.9-4.0, 7.8-13.3	Cohen 1984
GL 2392	2.1-2.5, 2.9-4.0, 7.8-13.3	Cohen 1984
GL 2310	2.1-2.5, 2.9-4.0, 8.0-13.2	Merrill and Stein 1976b
<u>AGB CI 09</u>		
+10216/GL 1381	1.8-2.6, 2.8-5.5 2.0-8.5 7.8-13.2 15.7-30	Strecker (unpublished) Witteborn et al. 1980 Cohen 1984 Forrest, Houck, and McCarthy 1981

GL 3116	31-180	Goebel and Moseley 1985
	2.1-2.5, 2.9-4.0,	
	7.8-13.3	Cohen 1984
	15.8-30	Forrest, Houck, and McCarthy 1981
<u>AGB CI 11</u>	used average of AGB CI 11 and 13	
<u>AGB CI 13</u>		
GL 2699	2.1-2.5, 2.9-4.0,	
	7.8-13.3	Cohen 1984
GL 3099	2.1-2.5, 2.9-4.0,	
	7.8-13.4	Cohen 1984
<u>AGB CI 15</u>	used photometry, LRS, and blackbody	
<u>AGB CI 17</u>		
GL 3068	2.1-2.5, 2.9-3.6,	
	8-13.4	Jones et al. 1978
	8.0-13.4	Cohen 1984
	15.8-30	Forrest, Houck, and McCarthy 1981
	31-150	Goebel and Moseley 1985
<u>AGB CI 19</u>	used photometry, LRS, and blackbody	
<u>AGB CI 21</u>	taken equal to AGB CI 19 template	
<u>AGB CI 23</u>	taken equal to AGB CI 19 template	
<u>AGB CI 25</u>	taken equal to AGB CI 19 template	
<u>AGB CI 27</u>	taken equal to AGB CI 19 template	
<u>AGB CI 29</u>	taken equal to AGB CI 19 template	
<u>AGB CI 31</u>	taken equal to AGB CI 19 template	
<u>X 1E</u>		
S Per	1.2-2.6, 2.6-4.0	Strecker (unpublished)
GL 1992	1.4-1.8, 2.0-2.5	Jones et al. 1988
GL 2019	1.4-1.8, 2.0-2.5	Jones et al. 1988
<u>X 1A</u>		
OH 327.4-0.6	1.4-1.8, 2.0-2.5	Jones et al. 1988
OH 30.7+0.4		used photometry, LRS, and 2 blackbodies
OH 32.0-0.5		used photometry, LRS, and 2 blackbodies
OH 32.8-0.3		used photometry, LRS, and 2 blackbodies
OH 75.3-1.8		used photometry, LRS, and 2 blackbodies
<u>X 2</u>		
GL 2136	1.6-2.5, 2.8-4.1,	
	4.5-13.4	Willner et al. 1982
	5.3-8.0	Tielens (unpublished)
<u>X 3</u>		
OH 21.5+0.5		used photometry, LRS, and 2 blackbodies
GL 2403		used photometry, LRS, and 2 blackbodies
<u>X 4</u>		
VY CMa	1.2-2.6, 2.6-4.0	Strecker (unpublished)
	5.2-10.2	Cohen et al. 1989

	15.8-30.3	Forrest, McCarthy, and Houck 1979
	20.0-35.1	Glaccum 1990
+10420	7.9-13.2	Giguere, Woolf, and Webber 1976
	15.6-38.5	Forrest, McCarthy, and Houck 1979
	19.9-35.0	Glaccum 1990
OH 337.9+0.2	1.4-1.8, 2.0-2.5	Jones et al. 1988
<u>X 5</u>		
MWC 300	2.1-2.5, 2.8-4.1	Cohen 1975
OH 127.8-0.0		used photometry, LRS, and 2 blackbodies
<u>PN BLUE</u>		
BD+30 3639	2.1-2.5, 2.9-4.1	Russell, Soifer, and Merrill 1977
	5.3-8.1	Cohen et al. 1986
	7.9-13.3	Aitken and Roche 1982
M2-56	2.1-2.5, 2.9-4.0	Eiroa, Hefele, and Zhang-Yu 1983
	5.4-8.0	Cohen (unpublished)
	8.1-13.5	Roche and Aitken 1986
GL 618	2.1-2.5, 2.8-4.0,	
	4.5-13.1	Russell, Soifer, and Willner 1978
<u>PN RED</u>		
NGC 6302	1.9-2.5	Ashley and Hyland 1988
	3.0-3.8	Magazzu and Strazzulla 1989
	5.3-7.9	Cohen et al. 1989
	7.4-13.5	Roche and Aitken 1986
NGC 6572	2.1-2.5, 2.9-4.1,	
	5-14	Willner et al. 1979
	1.9-2.4	Isaacman 1984
	1.3-3.6	Witteborn and Bregman (unpublished)
	5.3-8.1	Cohen et al. 1986
	8.1-13.3	Aitken and Roche 1982
	16.5-29.5	Forrest, Houck, and McCarthy 1981
NGC 7027*	2.1-2.5, 2.9-4.1,	
	4.5-13.8	Russell, Soifer, and Willner 1977
	15.7-38.5	McCarthy, Forrest, and Houck 1978
IC 418	2.1-2.5, 2.9-4.1,	
	5-14	Willner et al. 1979
	2.1-2.5, 2.9-4.1	Russell, Soifer, and Merrill 1977
	5.3-8.0	Cohen et al. 1986
	16.6-28.5	Forrest, Houck, and McCarthy 1981
Hb 5	3.0-3.8	Magazzu and Strazzulla 1989
	8-13	Aitken and Roche 1982
IC 2621	3.0-3.8	Magazzu and Strazzulla 1989
	8-13	Aitken and Roche 1982
He 2-131	3.0-3.8	Magazzu and Strazzulla 1989
	8-13	Aitken and Roche 1982
IC 4997		used photometry, LRS, and 2 blackbodies
NGC 7026		used photometry, LRS, and 2 blackbodies
<u>RN BLUE</u>		
HD 44179	1.2-2.6, 2.9-5.5	Strecker (unpublished)
	2.1-2.5, 2.8-4.0,	
	4.5-13	Russell, Soifer, and Willner 1978
	5.2-12.8	Cohen et al. 1986

NGC 2023	1.2-2.5, 2.8-3.7, 5.2-8.0, 8.7-12.9	Sellgren et al. 1985
<u>RN RED</u>		
NGC 7023	1.2-2.5, 2.8-4.2, 5.2-8.0, 8.7-11.8	Sellgren et al. 1985
Parsamyan 18	2.1-2.3 3.1-3.8 5.2-8.0	Sellgren 1986 Geballe (unpublished) Witteborn, Bregman, Cohen (unpublished)
<u>HII REG</u>		
GL 2591	2.1-2.5, 2.8-4.1, 4.5-13.4	Willner et al. 1982
W3 IRS5	2.0-2.5, 2.8-4.1, 4.5-13.4	Willner et al. 1982
[M1-78]	2.0-2.5 5.3-8.1 8.2-13.4	Isaacman 1984 Cohen et al. 1986 Aitken and Roche 1982
NGC 7538 IRS1	1.6-2.5, 2.8-4.1, 4.5-13.6	Willner et al. 1982
NGC 7538 IRS9	1.6-2.5, 2.8-4.1, 4.5-13.6	Willner et al. 1982
NGC 2170 IRS3	1.2-2.5, 2.8-4.1, 4.5-13.6	Willner et al. 1982
GL 2059	1.7-2.5, 2.8-4.1, 4.5-13.6	Willner et al. 1982
GL 961	1.7-2.5, 2.8-4.1, 4.5-13.6	Willner et al. 1982
GL 989	2.1-2.5, 2.8-4.1, 4.5-13.5	Willner et al. 1982
S 255 IRS 1	1.7-2.5, 2.8-4.1, 4.5-13.6	Willner et al. 1982
OMC2 IRS3*	1.6-2.5, 2.8-4.1, 4.5-13.5	Willner et al. 1982
GL 2884/S140	1.3-2.5, 2.8-4.1, 4.5-13.5	Willner et al. 1982
<u>T TAURI</u>		
HL Tau	2.1-2.5, 2.9-4.1 5.4-8.1 8.0-13.0	Cohen 1975 Witteborn and Bregman (unpublished) Cohen and Witteborn 1985
RY Tau	2.1-2.5, 2.9-4.1 8.0-13.0	Cohen 1975 Cohen and Witteborn 1985
GW Ori	2.1-2.5, 2.9-4.1 8.0-12.8	Cohen 1975 Cohen and Witteborn 1985
R Mon	2.1-2.5, 2.9-4.1 7.8-13.4	Cohen 1975 Cohen 1980
AB Aur	2.1-2.5, 2.9-4.1 8.0-13.0	Cohen 1975 Cohen and Witteborn 1985
<u>Galaxies</u>		
M82	1.7-2.5, 2.9-4.1, 5.4-13 16.0-30.3, 30-39 18.6-18.8, 33.3-.5	Willner et al. 1977 Houck, Forrest, and McCarthy 1980 Houck et al. 1984

NGC 1068	1.2-2.5, 2.8-4.1,	Cutri et al. 1981 Houck, Forrest, and McCarthy 1980 Russell, Soifer, and Merrill 1977 Witteborn, Bregman, Cohen (unpublished)
	8.1-13.4	
	16.5-29.7	
NGC 253	2.9-4.0	
	5.3-8.0	

Table 2. Breakdown of the assembled database of spectral fragments by wavelength region (in μm).

	$\lambda\lambda$ 1/2-4/5	5-8	8-13	LRS (7.7-22.7)	15-30	30-50
Number	144	43	71	168	34	22
Site	ground	air	ground	IRAS satellite	air	air